

1 **The Imminent Data Desert: The Future of Stratospheric Monitoring in**
2 **a Rapidly Changing World**

3 Ross J. Salawitch,^a Jessica B. Smith,^b Henry Selkirk,^{c,d} Krzysztof Wargan,^{e,f}
4 Martyn P. Chipperfield,^g Ryan Hossaini,^h Pieter F. Levelt,^{i,j,k} Nathaniel J. Livesey,^l
5 Laura A. McBride,^m Luis F. Millán,^l Elisabeth Moyer,ⁿ Michelle L. Santee,^l
6 Mark R. Schoeberl,^m Susan Solomon,^o Kane Stone,^o Helen M. Wordenⁱ

7 ^a*University of Maryland, College Park, MD*

8 ^e*Harvard University, Cambridge, MA*

9 ^c*NASA Earth Science Division, Washington, DC*

10 ^d*Agile Decision Sciences, Falls Church, VA*

11 ^e*NASA Goddard Space Flight Center, Greenbelt, MD*

12 ^f*Science Systems and Applications Inc., Lanham, MD*

13 ^g*University of Leeds, Leeds LS2 9JT, United Kingdom*

14 ^h*Lancaster University, Lancaster, United Kingdom*

15 ⁱ*NSF National Center for Atmospheric Research, Boulder, CO*

16 ^j*Royal Netherlands Meteorological Institute, De Bilt, The Netherlands*

17 ^k*University of Technology Delft, The Netherlands*

18 ^l*Jet Propulsion Laboratory, California Institute of Technology, Pasadena, CA*

19 ^m*Science and Technology Corporation, Columbia, MD*

20 ⁿ*University of Chicago, Chicago, IL*

21 ^o*Massachusetts Institute of Technology, Cambridge, MA*

22 Corresponding author: Ross J. Salawitch, rsalawit@umd.edu

23 ABSTRACT

24 The Atmospheric Chemistry Experiment-Fourier Transform Spectrometer (ACE-FTS) on
25 SCISAT-1 and Microwave Limb Sounder (MLS) on NASA's Aura satellite have contributed
26 significantly to understanding the impacts of human activities on the stratospheric ozone
27 layer. The two-decade-long data record from these instruments has allowed quantification of
28 ozone depletion caused by human-released ozone-depleting substances, the effects of extreme
29 natural events like major volcanic eruptions including Hunga in 2022, as well as events
30 amplified by human-caused climate change such as wildfires that inject material into the
31 stratosphere, as happened over Australia in early 2020. The Aura platform is nearing the end
32 of its operational lifetime and SCISAT-1 is over 20 years old. Their decommissioning will
33 cause a substantial gap in the measurement of critical atmospheric components, including
34 water vapor, inorganic chlorine species, and tracers of stratospheric transport. This upcoming
35 "data desert" poses significant challenges for monitoring the recovery of the ozone layer and
36 assessing the effects on stratospheric composition of future extreme events, threats posed by
37 increases in space debris from satellite burn-up, and the possible injection of stratospheric
38 aerosol to mitigate global warming. The lack of confirmed future missions that can provide
39 daily near-global profile measurements of stratospheric composition highlights the need for
40 observational strategies to bridge this impending gap. This paper discusses the essential role
41 of ACE-FTS and MLS in advancing our understanding of the stratosphere, the impact of data
42 loss after the cessation of one or both instruments, and the urgency of developing strategies
43 for mitigating the impact of these observational losses at a time marked by dramatic changes
44 in the stratosphere due to human and natural factors.

45 SIGNIFICANCE STATEMENT

46 We highlight the critical role that data from the ACE-FTS and MLS satellite instruments
47 have played in advancing our understanding of stratospheric composition and the impacts of
48 human activities on the ozone layer. As these instruments near the end of their operational
49 lifetimes, the imminent loss of data, particularly of stratospheric water vapor, chlorine
50 species, and tracers of transport, portends profound and irrevocable gaps in atmospheric
51 observations. This loss of observational capability will occur at a time of rapid climate
52 change and hinder our understanding of the stratosphere's response to, and its coupled role in,
53 continued climate forcing. This paper emphasizes the urgency of addressing this "data

54 desert," highlighting the need for sustained, coordinated, global measurement capabilities for
55 these crucial constituents.

56 CAPSULE

57 Soon global daily stratospheric halogen and tracer measurements will be lost, limiting the
58 ability to quantify how stratospheric ozone and its climate impacts are altered by
59 anthropogenic and natural forcings.

60 **Introduction**

61 Earth's stratospheric ozone layer protects humans, animals, agriculture, and ecosystems
62 against the harmful effects of solar ultraviolet radiation (Madronich *et al.*, 1998; Bais *et al.*,
63 2018). Variations in stratospheric water vapor play an important role in climate change
64 (Solomon *et al.*, 2010; Dessler *et al.*, 2013). Since their respective launches in 2003 and
65 2004, data from the Atmospheric Chemistry Experiment-Fourier Transform Spectrometer
66 (ACE-FTS) instrument on the Canadian Space Agency SCISAT-1 satellite (Bernath *et al.*,
67 2005) and the Microwave Limb Sounder (MLS) instrument on the NASA Aura satellite
68 (Waters *et al.*, 2006) have been essential to the global atmospheric science community's
69 efforts to quantify the impacts of human activity and extraordinary natural events on Earth's
70 ozone layer and stratospheric composition and chemistry more broadly. Measurements
71 acquired by ACE-FTS and MLS have enabled quantification of how the ozone layer has been
72 altered by the human release of chlorofluorocarbons (CFCs) and other ozone-depleting
73 substances (ODSs) regulated by the Montreal Protocol (Mahieu *et al.*, 2014; Livesey, Santee
74 and Manney, 2015; Bernath and Fernando, 2018), by natural factors such as the eruption of
75 the undersea volcano Hunga in 2022 (Millán *et al.*, 2022; Xu *et al.*, 2022; Santee *et al.*, 2023;
76 Wilmouth *et al.*, 2023), by extreme events such as the Australian wildfires of late 2019 and
77 early 2020 (Schwartz *et al.*, 2020; Santee *et al.*, 2022; Strahan *et al.*, 2022; Solomon *et al.*,
78 2023), and during winter-spring periods with long-lasting cold conditions in the Arctic
79 stratosphere that lead to severe ozone depletion (Manney *et al.*, 2011, 2020; Griffin *et al.*,
80 2019; Lawrence *et al.*, 2020; Wohltmann *et al.*, 2020; Feng *et al.*, 2021; Groß and Müller,
81 2021). Furthermore, data from these satellite instruments have been instrumental in
82 quantifying how long-term changes in stratospheric water vapor impact surface climate
83 (Solomon *et al.*, 2010; Banerjee *et al.*, 2019; Tao *et al.*, 2023) and for diagnosing changes in
84 the strength of the Brewer-Dobson circulation (BDC), which alters the latitudinal distribution
85 of stratospheric ozone (Strahan *et al.*, 2020; Minganti *et al.*, 2022; Prather *et al.*, 2023).

86 Aura will be decommissioned no later than the middle of 2026, and SCISAT-1 is 18 years
87 beyond its design lifetime. While there will remain considerable capability to measure
88 stratospheric profiles of O₃ and aerosols after these two missions end, the history of ozone
89 research demonstrates that understanding changes in the ozone layer requires measurements
90 of other species. There are no currently confirmed future space-borne missions to measure,
91 for example, the abundances of inorganic chlorine and nitrogen species such as ClO,

92 ClONO₂, HCl, and HNO₃ that are essential for relating the emissions of ODSs at the Earth's
93 surface to changes in the thickness of the ozone layer (WMO, 2022). Future daily near-global
94 profile measurements of stratospheric H₂O as well as tracers of stratospheric transport such as
95 N₂O or CH₄ will be important for diagnosing changes in the strength of the BDC (Strahan *et al.*,
96 2020; Minganti *et al.*, 2022; Prather *et al.*, 2023), but they also face an uncertain future.
97 The current scientific consensus is that an increase of the BDC with global warming should
98 lead to an accelerated recovery of total column ozone (TCO) at mid-latitudes of both
99 hemispheres, as well as a permanent reduction of TCO in the tropics that will result in
100 increased exposure at the surface to harmful solar ultraviolet radiation (Butchart *et al.*, 2006,
101 2011; Garcia and Randel, 2008; Abalos *et al.*, 2021). Finally, climate models (Smalley *et al.*,
102 2017; Keeble *et al.*, 2021) and theory (Hu and Vallis, 2019) predict a future rise in
103 stratospheric H₂O due to increases in the temperature of the tropical tropopause associated
104 with global warming. Should the future abundance of stratospheric H₂O rise appreciably
105 relative to present-day levels, declines in TCO would likely occur in both mid-latitudes
106 (Dvortsov and Solomon, 2001; Anderson and Clapp, 2018) and northern polar regions (Kirk-
107 Davidoff *et al.*, 1999; von der Gathen *et al.*, 2021). Finally, stratospheric ozone and water
108 vapor are both greenhouse gases important for climate change, and accurate quantification of
109 future climate change is a coupled chemistry-climate problem (IPCC, 2021).

110 This article provides an overview of current and potential future stratospheric
111 composition measurement capabilities. The discussion is organized in terms of H₂O, halogens
112 (e.g., ClO, ClONO₂, and HCl), tracers of stratospheric transport (N₂O, CH₄) and
113 anthropogenic pollution (e.g., HCN, CO, CH₃Cl), ozone, and aerosol loading. We highlight
114 the loss of data coverage that will occur, particularly for H₂O as well as halogens and tracers,
115 once observations from MLS and ACE-FTS are no longer available – a time we term the
116 “imminent data desert for stratospheric composition”. We follow by providing numerous
117 examples attesting to the importance of measurements from ACE-FTS and MLS for our
118 current understanding of how human activity and extreme natural events have affected the
119 ozone layer, both to document the vital role data from each platform has played and to
120 highlight the observational capability that will be lost once data from these instruments no
121 longer exist. Although we focus here on halogens, we note that space-borne instruments also
122 provide observations of many other species important for stratospheric ozone depletion, such
123 as nitrogen oxides that are supplied to the stratosphere by the decomposition of N₂O. Finally,
124 we conclude by noting the irony that the world's observational capability for diagnosing how

125 the ozone layer is being altered by human and natural factors will diminish at the same time
126 that mitigation of climate change by stratospheric aerosol injection – which poses a risk to the
127 future recovery of stratospheric ozone – is the subject of increasing research and dialogue
128 (NAS, 2015; NAS, 2021; Haywood *et al.*, 2022; Bednarz *et al.*, 2023; Tilmes *et al.*, 2024).

129 **Present And Future Measurement Capabilities**

130 Figure 1 shows a timeline of space-borne observational capability for the profiling of
131 stratospheric constituents by limb and occultation sounders over the past few decades, as well
132 as the planned capability provided by currently confirmed future missions. The thickness of
133 the bars represents the spatial density of observations, which is dependent upon observational
134 technique, as shown schematically in Figure 2. Solar occultation instruments typically
135 provide slightly finer vertical resolution and better single-sounding precision than limb
136 instruments, at the expense of much sparser spatial coverage. Ozone and aerosol observations
137 from the Ozone Mapping and Profiler Suite - Limb Profiler (OMPS-LP) series of limb-
138 scattering instruments (Jaross *et al.*, 2014; Loughman *et al.*, 2018) and the Stratospheric
139 Aerosol and Gas Experiment III instrument onboard the International Space Station (SAGE-
140 III/ISS) (Wang *et al.*, 2020) should provide continuity into the future. In contrast, future
141 measurements of stratospheric H₂O will be limited. SAGE-III/ISS provides high-vertical-
142 resolution measurements of the volume mixing ratio (VMR) of stratospheric water vapor
143 (Davis *et al.*, 2021). However, SAGE-III/ISS measurements are geographically and
144 temporally limited, and the continuation of instruments on the International Space Station
145 beyond 2030 is uncertain. The planned NASA/Naval Research Laboratory Gas Filter
146 Correlation Radiometer for Limb Occultation demo for upper atmosphere Temperature
147 (GLOTemp) and ESA Atmospheric Limb Tracker for the Investigation of the Upcoming
148 Stratosphere (ALTIUS) missions will use the solar occultation technique, similar to SAGE-
149 III/ISS but in a different orbit, again yielding sampling that is much sparser than is currently
150 achievable by limb emission and limb scattering instruments (Fig. 2). The situation for
151 observations of stratospheric water vapor should improve significantly with the launch of the
152 Canadian High Spectral Resolution Lidar for Aerosols, Winds, and Clouds (HAWC) mission
153 in 2030, four to five years after the end of the MLS record. Finally, there are presently no
154 confirmed plans to obtain daily near-global coverage of halogenated species (e.g., ClO,
155 ClONO₂, HCl), tracers of stratospheric transport (e.g., N₂O, CH₄), or anthropogenic pollution

156 (e.g., HCN, CO, CH₃Cl), all of which are essential ingredients for quantifying the impact on
 157 the ozone layer of ODSs and other pollutants.

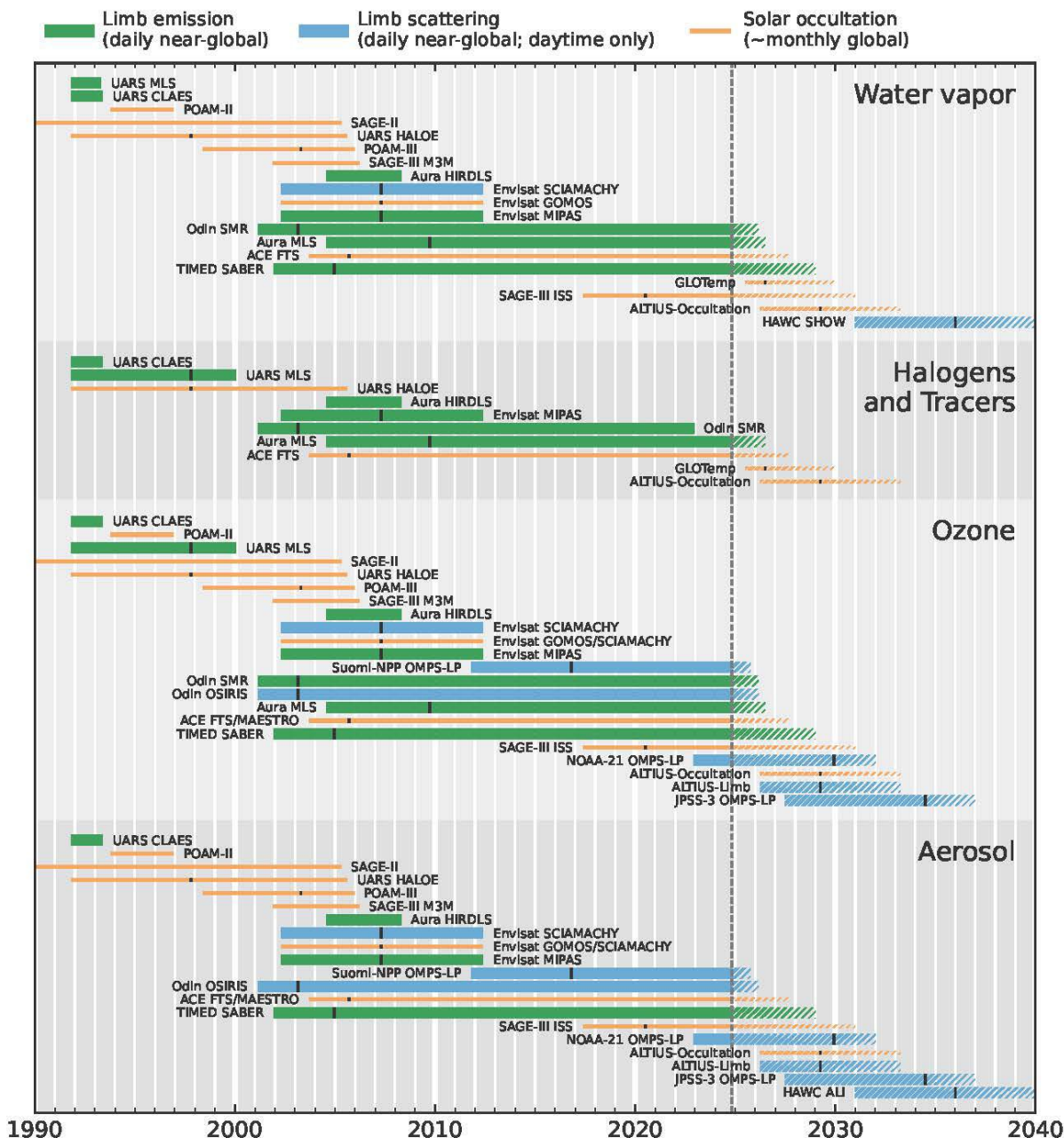


Figure 1. Space-borne limb or solar occultation observations of water vapor, halogens and tracers, ozone, and aerosol loading from 1990 to present, as well as projected future measurements considering currently confirmed missions. Colors denote observational technique, whereas line thickness qualitatively represents the observational density (see Figure 2). The thin black lines represent the end date of the design lifetime of the missions. The hashing represents the uncertainty in end dates of current satellite missions as well as uncertainty in future launch dates, and the vertical dashed line represents present time at paper submission.

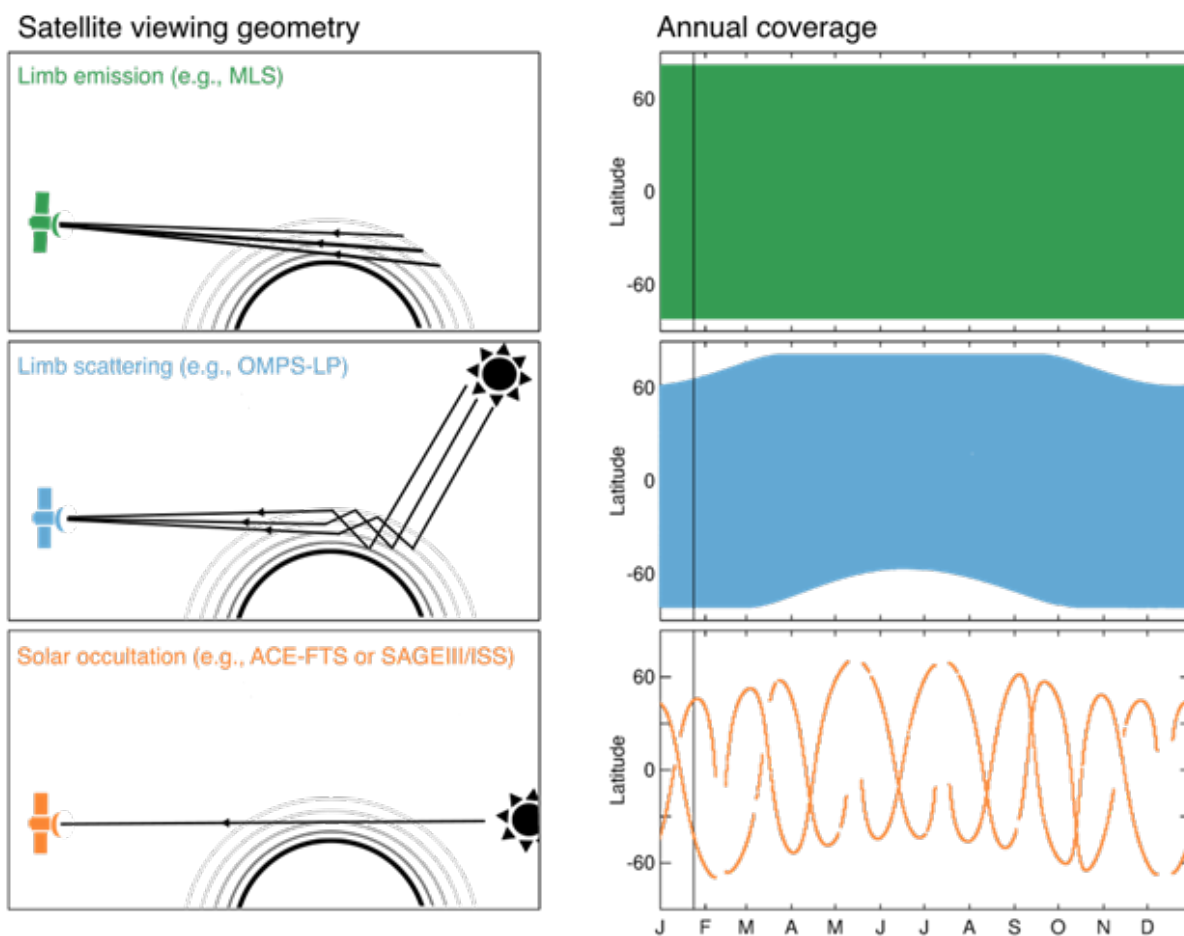


Figure 2. Satellite viewing geometry and consequent annual coverage for measurements obtained either using limb emission, limb scattering, or solar occultation. The panels on the right show the density of annual coverage from MLS on Aura, the Ozone Mapping and Profiler Suite - Limb Profiler (OMPS-LP), and the Stratospheric Aerosol and Gas Experiment III instrument on board the International Space Station (SAGE-III/ISS).

159 The left-hand side of Figure 3 illustrates the present observational capability for
 160 stratospheric constituents afforded by the current fleet of instruments, and the right-hand side
 161 shows the measurement coverage that will exist in the future. The top row depicts Arctic
 162 polar views for a typical boreal winter day in mid-January, the middle three rows highlight
 163 global coverage for a typical boreal spring day in mid-April, and the bottom row depicts
 164 Antarctic polar views for a typical austral winter day in mid-July. The current fleet provides
 165 dense coverage of H₂O, halogens, transport and pollution tracers, and ozone over the tropical
 166 and mid-latitude regions of the globe as well as throughout the Arctic and Antarctic. After
 167 cessation of MLS and ACE-FTS observations there will be limited coverage of the Arctic
 168 stratosphere during early boreal winter; similar gaps will exist over the Antarctic during the
 169 incipient phase of the annually occurring ozone hole in austral winter. The space-based

170 observational system will continue to be supplemented by data from sub-orbital instruments
 171 as shown in Figure 3. These include balloons carrying ozonesondes and frostpoint
 172 hygrometers (Thompson *et al.*, 2004; Hurst *et al.*, 2011; Stauffer *et al.*, 2022), ozone and
 173 aerosol lidars (Leblanc and McDermid, 2000; Chouza *et al.*, 2020; Steinbrecht *et al.*, 2023),
 174 as well as the Network for the Detection of Atmospheric Composition Change (NDACC)
 175 sites (De Mazière *et al.*, 2018) with Fourier Transform Infrared (FTIR) spectrometers that
 176 measure the total column abundance of a suite of gases including many halogens (Mahieu *et al.*
 177 *et al.*, 2014; Prignon *et al.*, 2021) and tracers of stratospheric transport (Ostler *et al.*, 2016;
 178 Minganti *et al.*, 2022) and microwave radiometers that quantify profiles of stratospheric H₂O
 179 (Nedoluha *et al.*, 2023) and ClO (Connor *et al.*, 2013).

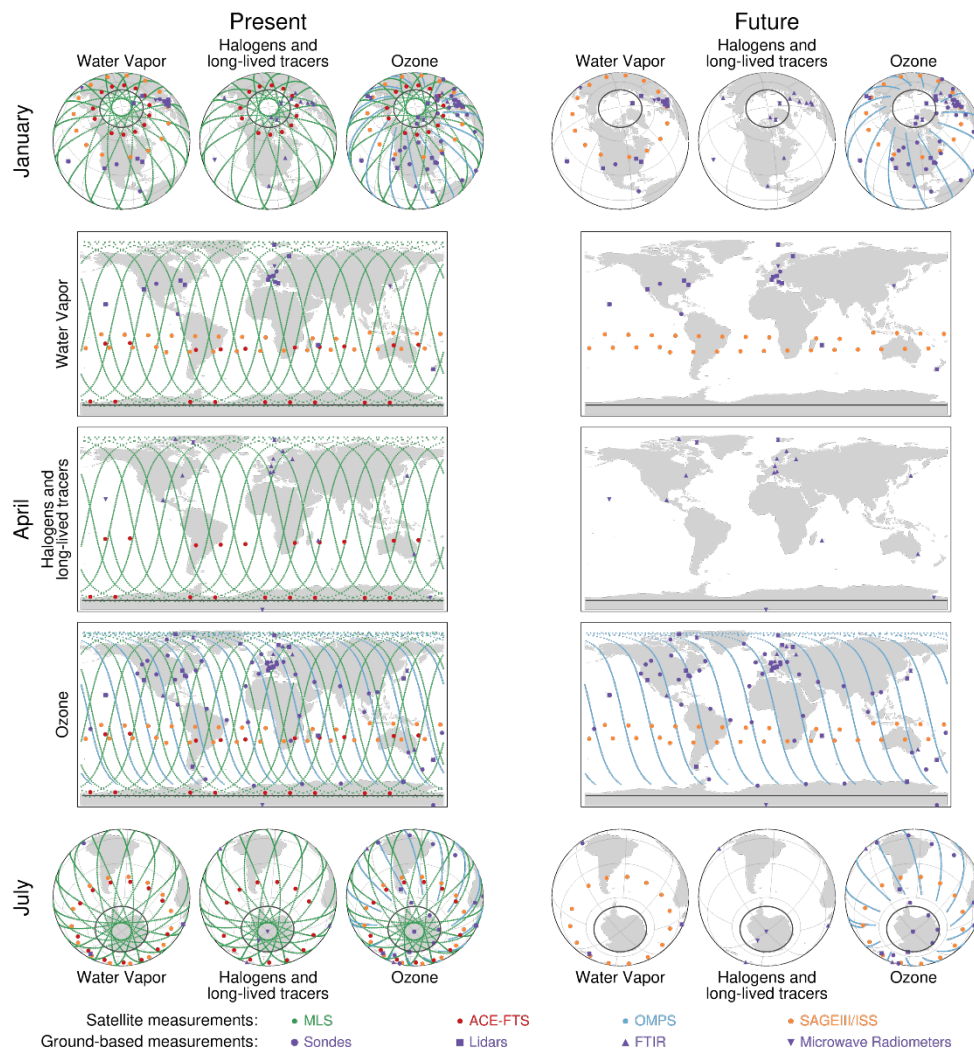


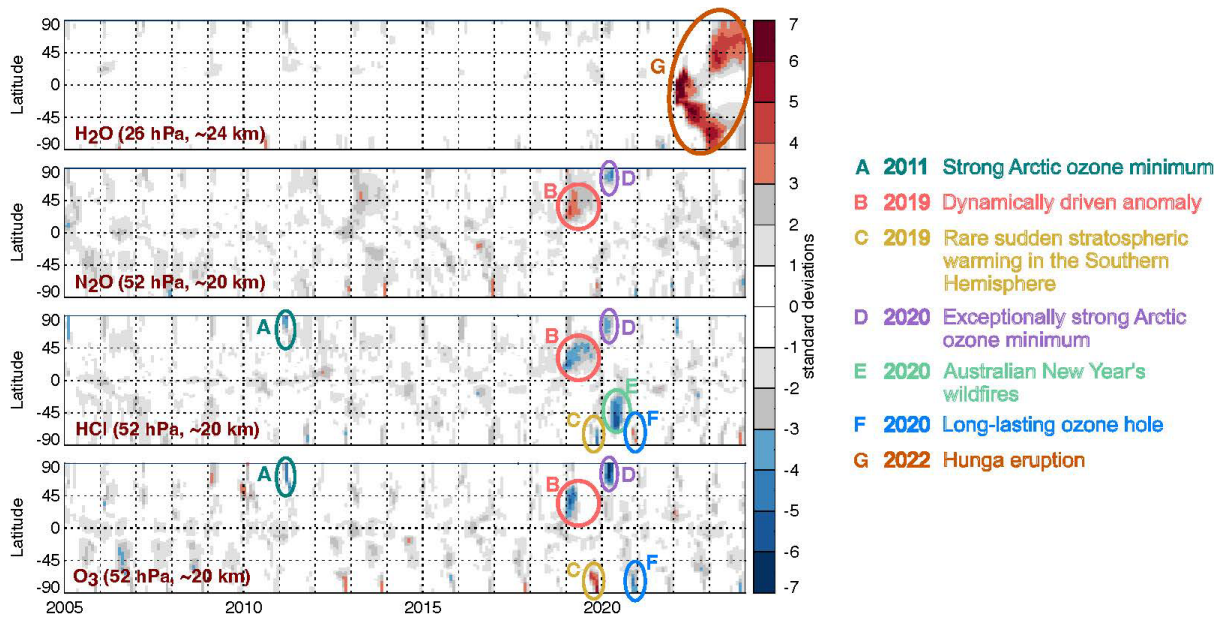
Figure 3. Observational density of vertically resolved measurements of stratospheric water vapor, halogens and tracers, and ozone at present (left) and in the future once MLS and ACE-FTS are no longer able to provide observations (right). Symbols correspond to various satellite and ground-based sensors (see legend); the black lines demarcate the boundary of polar night for the Arctic and Antarctic. For illustrative purposes, maps are shown for a representative days in mid-January, mid-April, and mid-July for the Arctic, Mercator, and Antarctic projection maps, respectively. These dates are chosen to highlight how well the current fleet of space-borne sensors, particularly MLS, can define initial conditions in the Arctic (top row) and Antarctic (bottom row) vortices in mid-winter, a time when chemical loss of ozone, which requires sunlight, has typically not commenced to a substantial degree in most of the vortex. The middle rows highlight the stark contrast between the current dense sampling capability and the sparse future measurement capability for a typical boreal spring day.

180

181 Over the past half-century, our understanding of stratospheric ozone has benefited
182 enormously from both space-borne and sub-orbital assets, including observations obtained by
183 the ground-based platforms highlighted in Fig. 3. However, sub-orbital instruments provide
184 limited sampling, and the use of these data is subject to influence from atmospheric
185 variability that must be overcome for accurate understanding of long-term trends (Hegglin *et al.*,
186 2014; Prignon *et al.*, 2021). Nonetheless, when observations from MLS and ACE-FTS
187 are no longer available, data from sub-orbital platforms will become critical to maintain and
188 possibly expand in terms of spatial and temporal sampling.

189 The Unusual Recent Stratosphere

190 The composition of Earth's stratosphere has been highly perturbed in recent years.
191 Figure 4 displays the interannual variability of H₂O, N₂O, HCl, and O₃ at selected pressure
192 levels in the stratosphere from 2005 through 2023. The detrended and deseasonalized VMR
193 anomalies in the figure were computed using the MERRA-2 Stratospheric Composition
194 Reanalysis of Aura MLS (M2-SCREAM) (Wargan *et al.*, 2023); anomalies greater than 3
195 standard deviations (σ) above the long-term mean are colored. Over the first 15 years, the
196 trace constituent anomaly time series show an expected degree of variability as the only
197 coherent set of 4σ and larger anomalies are those observed for O₃ and HCl during the cold
198 Arctic conditions in early 2011 ("A", Fig. 4). This 'business as usual' regime for
199 stratospheric composition ended in 2019, after which a series of 4σ and larger anomalies was
200 observed. Figure 5 presents the stratospheric aerosol optical depth (SAOD) over the same
201 time period as Figure 4, and it shows that many of the recent composition anomalies are
202 linked to large increases in SAOD, as explained in more detail below. The anomalies shown
203 in Figs. 4 and 5 serve as an organizational framework for the rest of this section.



204

Figure 4. Deseasonalized, detrended anomalies in time series of H₂O, N₂O, HCl, and O₃ mixing ratios at selected pressure levels, expressed in units of standard deviation from the mean (σ). Anomalies greater than 3σ deviation about the long-term mean are shown using color. Anomalies of 4σ or greater are circled and denoted by letters, with the geophysical event associated with each anomaly identified at right. The analysis is based on the M2-SCREAM assimilation of MLS observations driven by assimilated meteorological fields from MERRA-2 (Wargan *et al.*, 2023).

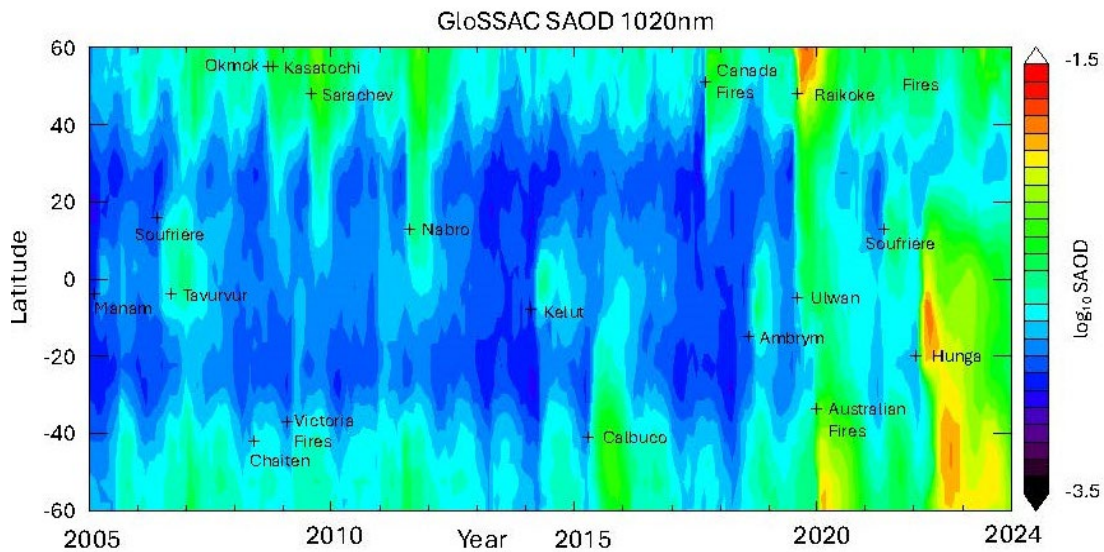


Figure 5. Variations in stratospheric aerosol optical depth (SAOD) at a wavelength of 1020 nm, computed based on integration of extinction coefficients from the Global Space-based Stratospheric Aerosol Climatology (GloSSAC) version 2.22 database (Thomason *et al.*, 2018; Kovilakam *et al.*, 2023). The impact of various volcanic eruptions and large wildfires on SAOD is evident, as marked.

205 A triad of 4σ and larger anomalies in O_3 , HCl, and N_2O was observed at Northern
206 Hemisphere (NH) mid-latitudes in 2019 (“B”, Fig. 4). These anomalies, first identified by
207 Manney *et al.*, 2022, are currently an active area of research and appear to be related to the
208 combination and relative timing of tracer transport by the secondary circulation associated
209 with the Quasi-Biennial Oscillation (QBO) in variations in the strength of stratospheric winds
210 and strong downward and poleward transport by the BDC in the winter of 2018/2019. Later
211 that year, a rare Southern Hemisphere (SH) sudden stratospheric warming occurred that was
212 associated with large anomalies in O_3 and HCl (“C”). Then in early 2020, unusually
213 prolonged cold conditions in the Arctic led to large anomalies in O_3 , HCl, and N_2O (“D”).
214 For the months following the Australian New Year’s fires that began in late 2019, a large
215 negative anomaly in HCl was observed throughout the SH mid-latitudes (“E”). The Antarctic
216 ozone hole in 2020 was exceptionally deep, with negative anomalies in O_3 and positive
217 anomalies in HCl (“F”). While 2021 was a relatively quiet year, the extraordinary eruption of
218 Hunga in January 2022 injected an enormous amount of water vapor deep into the SH
219 stratosphere and mesosphere, resulting in 4σ and larger anomalies in H_2O that began in the
220 tropics, expanded throughout SH mid-latitudes, and eventually reached both poles (“G”).

221 Many of these anomalies occur in polar regions and are observed for H_2O , N_2O , HCl,
222 and O_3 . As noted above, when ACE-FTS and MLS cease to operate, measurements of almost
223 all of these species will be extremely limited in the polar regions. Profiles of H_2O will be
224 sparse in both space and time for other regions of the stratosphere, and profiles of tracers
225 such as N_2O and halogens such as HCl, ClONO₂, and ClO will not exist for the global
226 stratosphere.

227 **Australian Wildfires.** The Australian wildfires of late 2019 and early 2020 injected massive
228 amounts of aerosol into the SH mid-latitude stratosphere (Fig. 5) (Khaykin *et al.*, 2020),
229 resulting in a reduction of TCO between 30°S and 60°S that reached its peak during May to
230 August 2020 at about 6 to 10 Dobson Units (DU) below the long-term mean (Rieger *et al.*,
231 2021; Strahan *et al.*, 2022). These wildfire aerosols warmed the stratosphere by several
232 degrees Celsius and resulted in a near-immediate alteration of stratospheric winds (Kablick
233 III *et al.*, 2020), which in turn led to dynamically induced reductions of TCO (Santee *et al.*,
234 2022; Strahan *et al.*, 2022). Declines in O_3 relative to N_2O served as the key observational
235 constraint for estimating the decline in TCO caused by changes in stratospheric transport.

236 Figure 6 shows observations of ClO and HCl from MLS and ClONO₂ from ACE-FTS
 237 in the SH mid-latitude stratosphere, with data collected in 2020 highlighted in red.
 238 Substantial enhancements of ClO and ClONO₂ are apparent, as is the suppression of HCl
 239 (Santee *et al.*, 2022; Strahan *et al.*, 2022). Models run with the standard hydrolysis of N₂O₅
 240 on sulfate aerosols and other heterogeneous processes that typically are important only under
 241 cold conditions failed to capture the magnitude of the observed response (Strahan *et al.*,
 242 2022). These enhancements in ClO are of the same magnitude as the increase that followed
 243 the 1991 eruption of Mount Pinatubo (Fahey *et al.*, 1993), and therefore are large enough to
 244 result in significant chemical loss of stratospheric ozone (Salawitch and McBride, 2022).
 245

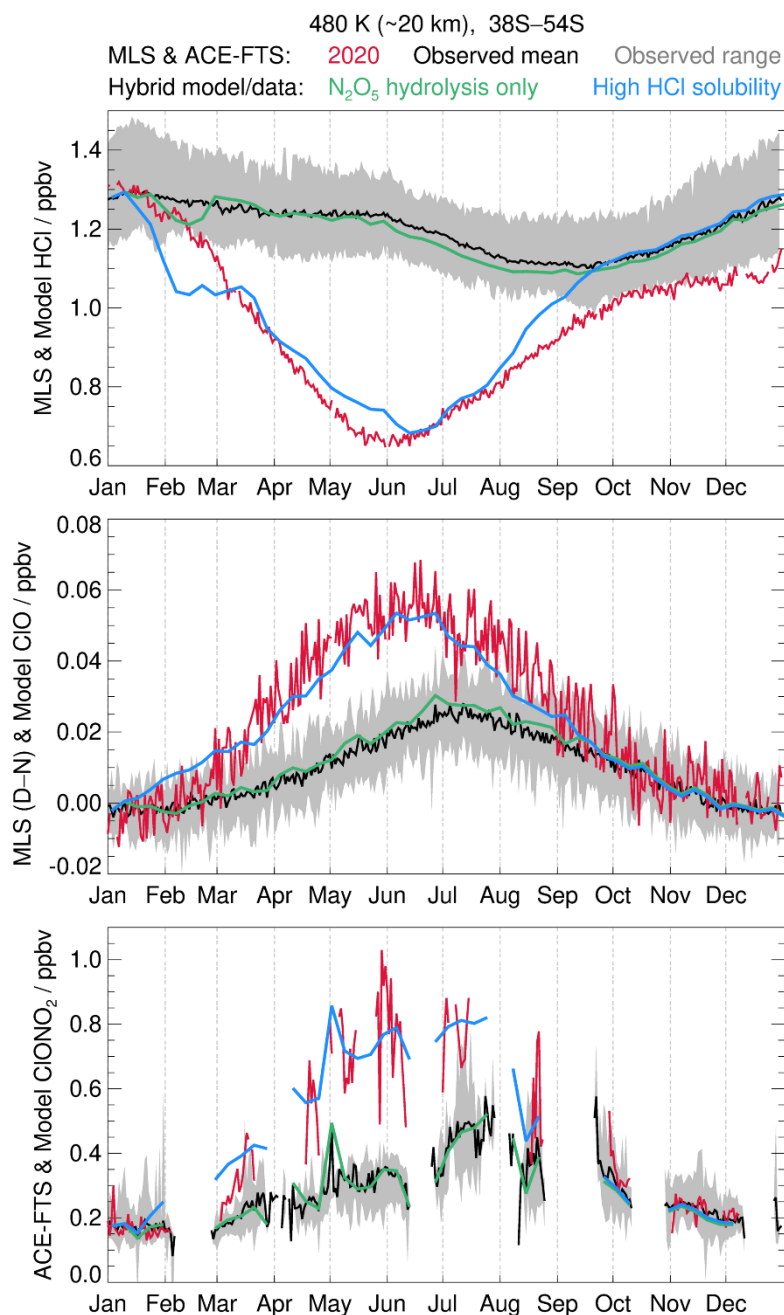


Figure 6. Daily (day and night) averaged mixing ratios of HCl, ClO, and ClONO₂ measured in 2020 (red), as well as the climatological mean (black) and range (grey) over 2005–2019 obtained by MLS (HCl and ClO) and ACE-FTS (ClONO₂) at the 480 K potential temperature level between 38°S and 54°S. For ClO, the 24-hour-averaged values are approximated as half of the day-night differences to reduce measurement biases (and assuming zero ClO at night). Also shown are hybrid modeled/measured quantities computed by adding model-calculated daily averaged anomalies in the three chlorine species to the respective observed climatological means from MLS and ACE-FTS. For the green lines, the anomalies are taken from a simulation using only N₂O₅ hydrolysis on aerosols and other heterogeneous processes in standard models; for the blue lines, they are taken from a simulation that includes enhanced solubility of HCl on organic aerosols and subsequent heterogeneous reactions of HCl. Adapted from Santee *et al.* (2022) and Solomon *et al.* (2023).

246 Solar infrared spectra obtained by ACE-FTS proved to be the key to explaining the
247 enhancements of ClO and ClONO₂ and suppression of HCl observed over broad regions of
248 the SH mid-latitude stratosphere in the months following the Australian wildfires. Bernath *et*
249 *al.* (2022) showed the presence of strong absorption features in SH mid-latitude spectra due
250 to C=O, CH, and OH stretching modes which are characteristic of organic aerosol. Solomon
251 *et al.* (2023) proposed that HCl would dissolve in these organic aerosols and undergo a series
252 of heterogeneous chemical reactions that could account for the observed reduction in HCl and
253 enhancements of ClONO₂ and ClO (blue lines, Fig. 6). Their model simulation accounting for
254 the dissolution and subsequent reaction of HCl shows that this chemical change, caused by
255 Australian wildfire aerosols, also contributed to the observed decline of TCO over broad
256 regions of the SH mid-latitude stratosphere.

257 The current consensus, summarized by Chipperfield and Bekki (2024), is that the
258 decline in TCO following the Australian wildfires was likely caused by a combination of
259 dynamics and chemistry. They also note that the physical state (that is, liquid, glassy, or
260 solid) and detailed composition of wildfire particles is not known and that future laboratory
261 measurements will be needed to advance our understanding of the impact of wildfires on
262 stratospheric composition. Nevertheless, observations provided by ACE-FTS and MLS
263 identified this critical – and unforeseen – chemical mechanism and were essential to
264 achieving our current level of understanding. If large wildfires continue to impact the
265 stratosphere during the future data desert, the causes of any resulting declines in stratospheric
266 ozone will be impossible to observationally determine due to the lack of high-spectral-
267 resolution infrared solar spectra along with few or no observations of ClO, ClONO₂, HCl,
268 and N₂O. This concern is heightened further by the likelihood that future drought and
269 changes in atmospheric stability due to global warming will lead to an increase in the

270 frequency of extreme wildfires, in Australia (Di Virgilio *et al.*, 2019) as well as in many other
271 fire-prone regions (Holden *et al.*, 2018; Pausas and Keeley, 2021).

272 Stratospheric circulation changes may also be causally linked to the Australian
273 wildfires. Studies have suggested that the hot, dry weather conditions in Australia during the
274 austral summer of 2019/2020 might, in part, be a response of the tropospheric climate system
275 to the weak stratospheric polar vortex in 2019 that is marked by the yellow circles (“C”) in
276 Fig. 4 (Lim *et al.*, 2019, 2021; Baldwin *et al.*, 2021). If a sudden stratospheric warming did
277 indeed foreshadow an event as catastrophic as the 2019/2020 Australian wildfires, then the
278 types of measurements discussed throughout this article could have a much greater impact
279 than is commonly appreciated.

280 **Hunga Eruption.** The eruption of the undersea Hunga Tonga-Hunga Ha’apai (Hunga)
281 volcano (20.54°S, 175.38°W) on 15 January 2022 injected enormous amounts of H₂O into
282 the stratosphere along with significant amounts of SO₂ (Khaykin *et al.*, 2022; Millán *et al.*,
283 2022; Vömel, Evan and Tully, 2022). MLS stratospheric H₂O profiles revealed that the mass
284 of H₂O injected into the stratosphere by this eruption was equivalent to about 10% of the
285 mass of H₂O present in the global stratosphere prior to the eruption. This amount vastly
286 exceeds the injection of H₂O by other volcanoes over the modern satellite record (1979 to
287 present) (Millán *et al.*, 2022; Vömel, Evan and Tully, 2022). The unique nature of this event
288 was due to a combination of its large volcanic explosive index (VEI) of 5.8, as well as the
289 submarine setting of the eruption (Khaykin *et al.*, 2022; Witze, 2022).

290 The top panel of Fig. 4 shows that at the 26 hPa pressure level, the extreme
291 enhancement of H₂O was confined to the tropics for the first few months after the eruption,
292 then spread throughout SH mid-latitudes (Schoeberl *et al.*, 2022; Santee *et al.*, 2023;
293 Wilmouth *et al.*, 2023). However, the strong winds that define the Antarctic polar vortex
294 prevented penetration of the H₂O plume into the vortex during 2022 (Manney *et al.*, 2023).
295 MLS data in Figure 4 show that the progression of enhanced H₂O into polar regions of both
296 hemispheres occurred during 2023 (Santee *et al.*, 2024; Wohltmann *et al.*, 2024; Zhang *et al.*,
297 2024).

298 Figure 7 shows anomalies of stratospheric H₂O from 2005 to present in the tropics, as
299 recorded by MLS and SAGE-III/ISS. This record of stratospheric H₂O, termed the “tape
300 recorder” by Mote *et al.* (1996), is directly linked to the impact of variations of tropical
301 tropopause temperature on stratospheric humidity (Randel and Park, 2019; Konopka *et al.*,

302 2022; Millán *et al.*, 2024) as well as the strength and variability of the BDC (Flury, Wu and
303 Read, 2013). The ability to observationally define the perturbation to stratospheric H₂O by
304 MLS, which provides daily near-global measurements, stands in contrast to the relatively
305 sparse record provided by solar occultation instruments such as SAGE-III/ISS (see Figure 3),
306 which first sampled the Hunga plume 3 to 5 days after the eruption, then not again until day
307 23, and then on days 30 to 33.

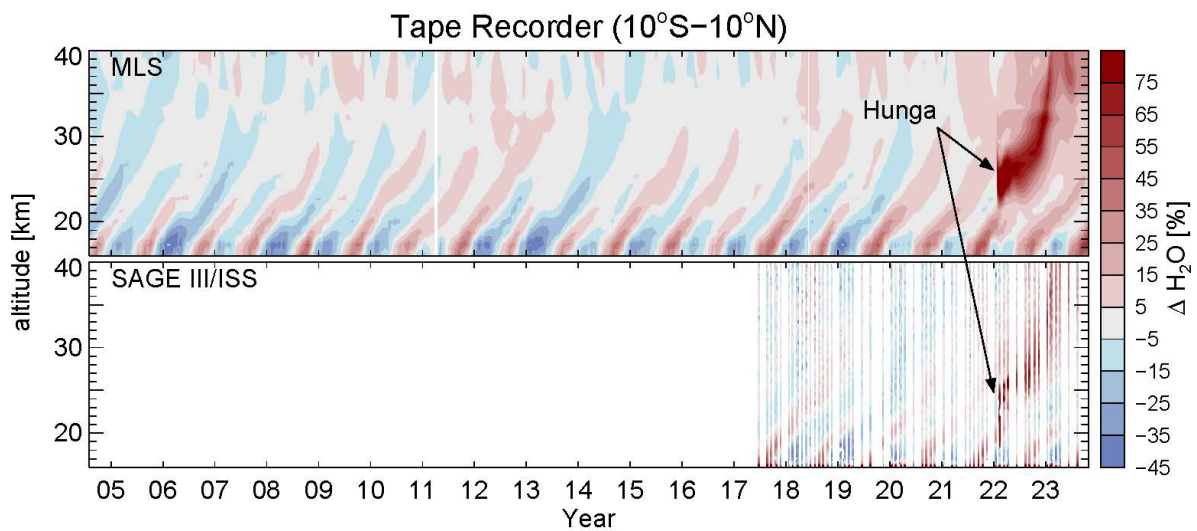


Figure 7. Zonal-mean H₂O anomalies (in percent) in the tropics (10°S–10°N), as a function of altitude and time, measured by Aura MLS and SAGE-III/ISS. Update to Figure 5 of Millán *et al.* (2022).

308 The Hunga eruption altered the temperature, transport, and chemistry of the
309 stratosphere in a manner that has been the subject of many recent studies. The impact of this
310 eruption on the characteristics of stratospheric aerosol loading has been well documented by
311 both balloon (Asher *et al.*, 2023; Evan *et al.*, 2024) and space-borne (Kloss *et al.*, 2022;
312 Legras *et al.*, 2022; Taha *et al.*, 2022; Knepp *et al.*, 2024) instruments that will continue to
313 operate for the foreseeable future, with the exception of the CALIOP space-borne lidar
314 onboard the NASA CALIPSO satellite, which ceased operations on 1 August 2023 after a
315 remarkable 17-year journey of discovery. Stratospheric lidar aerosol measurements will
316 continue with the ESA Earth Cloud, Aerosol and Radiation Experiment (EarthCARE)
317 (Illingworth *et al.*, 2015) that began operations in 2024.

318 However, quantitative understanding of the impact of the Hunga eruption on
319 stratospheric O₃ has relied on analyses of data acquired by MLS and ACE-FTS. Enhanced
320 levels of stratospheric H₂O resulted in a 2 to 3 K cooling throughout the global upper
321 stratosphere (Coy *et al.*, 2022; Schoeberl *et al.*, 2022; Wang *et al.*, 2023), with largest effects
322 in May 2022 of about 5 K cooling at 20 hPa between 20°S and 25°S (Fleming *et al.*, 2024).
323 Our theoretical understanding of the stratospheric cooling induced by the Hunga eruption is
324 guided by reanalyses and by models initialized with MLS profiles of H₂O (Coy *et al.*, 2022;
325 Wang *et al.*, 2023; Fleming *et al.*, 2024). As was the case for the Australian wildfires, the
326 reductions in extrapolar TCO that resulted from the Hunga eruption were due to a
327 combination of dynamical and chemical effects (Santee *et al.*, 2023; Wang *et al.*, 2023;
328 Wilmouth *et al.*, 2023; Fleming *et al.*, 2024). Analysis of monthly mean anomalies of VMRs
329 of O₃ versus N₂O at various latitudes and altitudes was the essential element for quantifying
330 the contribution of Hunga-induced changes in stratospheric transport to reductions in TCO
331 over broad regions of the SH (Santee *et al.*, 2023; Wilmouth *et al.*, 2023). Measurements of
332 stratospheric profiles of halogens and tracers from MLS and ACE-FTS also enabled
333 diagnosis of the effect of the Hunga eruption on stratospheric chemistry, both through
334 elevated OH due to the oxidation of H₂O, followed by enhancements of ClO due to the
335 reaction of OH with HCl (Zhu *et al.*, 2022, 2023; Wilmouth *et al.*, 2023; Fleming *et al.*, 2024;
336 Zhang *et al.*, 2024), and through heterogeneous chemistry on volcanic aerosols (Santee *et al.*,
337 2023; Zhang *et al.*, 2024). Impacts of the Hunga eruption on the Antarctic ozone hole have
338 also been investigated using measurements from MLS (Manney *et al.*, 2023; Fleming *et al.*,
339 2024; Santee *et al.*, 2024; Wohltmann *et al.*, 2024; Zhou *et al.*, 2024). Should an eruption
340 with a VEI approaching the magnitude of Hunga occur during the upcoming data desert, the

341 lack of profiles of halogens and tracers throughout the global stratosphere will hamper
342 quantification of the factors responsible for the associated changes to stratospheric
343 composition.

344 **Ozone Layer Recovery**

345 **Mid-Latitude Ozone.** The recovery of ozone from depletion by anthropogenic halogens is not
346 occurring as fast as had been expected, particularly for the NH mid-latitude lower
347 stratosphere (Ball *et al.*, 2018; Chipperfield *et al.*, 2018; Wargan *et al.*, 2018; Orbe *et al.*,
348 2020; Weber *et al.*, 2022; Bednarz, Hossaini and Chipperfield, 2023; Chipperfield and Bekki,
349 2024). Due to the success of the Montreal Protocol, the surface abundances of CFCs and
350 most other ODSs have been declining over the past two decades, and stratospheric halogen
351 loading started to decrease after the late 1990s (WMO, 2022). Everything else being equal, a
352 rise of TCO at NH mid-latitudes should have been observed over the past decade (Oman *et*
353 *al.*, 2010; Eyring *et al.*, 2013; Dhomse *et al.*, 2018; Keeble *et al.*, 2021). However, trends in
354 TCO between 35°N and 60°N have been negligible from 1996 to present (a change of $0.0 \pm$
355 0.7% decade⁻¹), in contrast to 35°S to 60°S, where TCO has been rising at a rate of $0.8 \pm$
356 0.7% decade⁻¹, close to the expected rate of recovery (WMO, 2022).

357 Several hypotheses have been advanced to explain the slower-than-expected recovery
358 of ozone at NH mid-latitudes. These include dynamical influences on ozone such as QBO
359 variations in the strength of stratospheric winds, structural changes in the BDC, and changes
360 in dynamical patterns such as the Arctic Oscillation (Ball *et al.*, 2018, 2020; Chipperfield *et*
361 *al.*, 2018; Wargan *et al.*, 2018; Coldewey-Egbers *et al.*, 2020; Orbe *et al.*, 2020). Chemical
362 effects such as the influence of a class of compounds called Very-Short Lived chlorocarbons
363 (VSL-Cl), which have rising emissions (Fang *et al.*, 2019; An *et al.*, 2021) and are not
364 regulated by the Montreal Protocol, have also been proposed as a factor in the delayed
365 recovery of ozone at NH mid-latitudes (Hossaini *et al.*, 2017, 2024; Chipperfield *et al.*, 2020;
366 Bednarz, Hossaini and Chipperfield, 2023; Villamayor *et al.*, 2023).

367 A comprehensive analysis of the total chlorine budget is an important element of our
368 ability to relate surface emissions of ODSs to the effect of these anthropogenic halogens on
369 the ozone layer. Nassar *et al.* (2006) examined ACE-FTS observations of a suite of organic
370 and inorganic chlorine species in five latitude bands over a variety of stratospheric altitudes
371 and concluded that there was evidence of an initial decline in global stratospheric chlorine in
372 2004 consistent with both stratospheric circulation and the time lag necessary for transport of
373 chlorine from the surface to the stratosphere. However, the rate of the decline in inorganic
374 chlorine in the upper stratosphere since 2004 is uncertain. Nearly the entire complement of
375 inorganic chlorine in the upper stratosphere is present as HCl. Bernath and Fernando (2018)
376 concluded based on linear regression analysis that upper stratospheric HCl between 60°S and
377 60°N, as measured by ACE-FTS, was declining over the period 2004 to 2017 in a manner
378 quantitatively consistent with the decline in surface abundances of CFCs and other ODSs
379 regulated by the Montreal Protocol. Conversely, Hossaini *et al.* (2019) and Bednarz *et al.*
380 (2022) analyzed similar measurements using global models and concluded that upper
381 stratospheric HCl is declining more slowly than expected based solely on long-lived ODSs,
382 as shown in Figure 8, and that trends in HCl measured by ACE-FTS are best explained by
383 allowing for the impact of the unregulated VSL-Cl gases on the stratospheric chlorine budget.

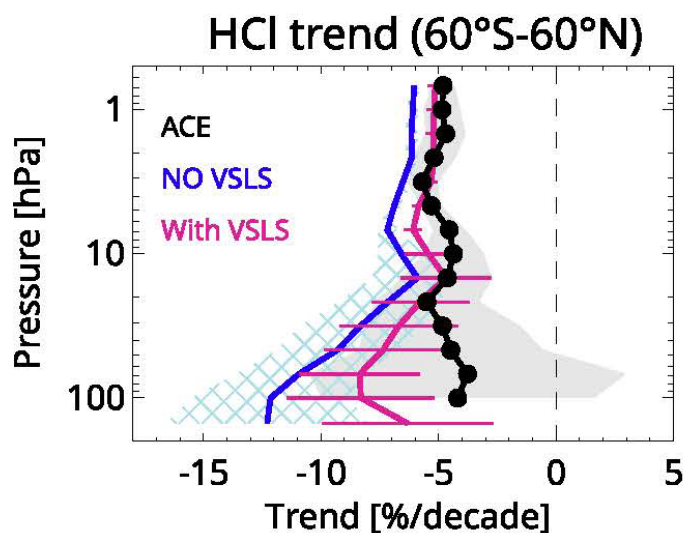


Figure 8. Impact of VSL-Cl on stratospheric HCl trends. Mean HCl trends (2004–2017) calculated for latitudes 60°S–60°N. Modelled HCl trends (% per decade) with and without VSL-Cl from the Toulouse Off-Line Model of Chemistry and Transport (TOMCAT) 3D chemical-transport model. For the long-lived chlorine source gases, the model used global mean surface mixing ratios based on observations. Observed HCl trends are derived from the ACE-FTS satellite instrument. 2σ trend uncertainties are denoted by the horizontal bars, shading, and hatching. The inclusion of VSL-Cl increases the HCl trend, especially in the lower stratosphere, bringing the model into better agreement with the observations.

384 Upper-stratospheric chlorine is currently measured by both MLS (Froidevaux *et al.*,
385 2006, 2022) and ACE-FTS (Bernath and Fernando, 2018). The future loss of these
386 measurements will impede our ability to connect changes in the surface abundances of CFCs,
387 other ODSs, and VSL-Cl to the ultimate driver of chemical loss of ozone, which is the
388 abundance of stratospheric chlorine. The impending data desert will occur at an especially
389 precarious time for monitoring the evolution of stratospheric chlorine because:

- 390 1) revisions to projections of future abundances of the 16 principal ODSs, due to
391 updates in leakage rates from allowed use as feedstock for the manufacture of
392 other compounds together with updates to the emissions from existing and future
393 equipment ('banks'), show that the future decline of stratospheric chlorine will be
394 considerably slower than previously expected (Lickley *et al.*, 2021, 2024; Li *et al.*,
395 2024);
- 396 2) ground-based observations reveal a rise in the atmospheric abundances of five
397 minor CFCs used mainly as feedstock for the production of other chemicals that,
398 should this rise continue, will counteract some of the benefits gained under the
399 Montreal Protocol (Western *et al.*, 2023);
- 400 3) the atmospheric abundances of most VSL-Cl gases, which are not regulated by the
401 Montreal Protocol, are continuing to rise (Fang *et al.*, 2019; Hossaini *et al.*, 2019,
402 2024; Chipperfield *et al.*, 2020; An *et al.*, 2021; Bednarz *et al.*, 2022; Villamayor
403 *et al.*, 2023)); and
- 404 4) airborne measurements, augmented by MLS observations of CO, show significant
405 transport to the stratosphere of five major VSL-Cl gases by the East Asian
406 summer monsoon, including the first quantification of stratospheric injection of
407 relatively large amounts of 1,2 dichloropropane (C₃H₆Cl₂) (Pan *et al.*, 2024).

408 As noted above, the strength of the BDC is projected to increase, which should
409 accelerate the recovery of TCO at mid-latitudes of both hemispheres and lead to a permanent
410 reduction of TCO in the tropics (Butchart *et al.*, 2006, 2011; Garcia and Randel, 2008;
411 Abalos *et al.*, 2021). During the imminent data desert, sporadic measurements of profiles of
412 transport tracers such as N₂O and CH₄ will likely not be sufficient to quantify how the BDC
413 is changing, a substantial limitation given the large range of theoretical projections of the
414 magnitude of the future increase in the strength of the BDC and the fact that the predicted
415 strengthening of the BDC has not yet been conclusively observed (Butchart *et al.*, 2006; Li,

416 Austin and Wilson, 2008; Abalos *et al.*, 2021). The picture is further complicated by the
417 chemical impacts of N₂O and CH₄, whose abundances are increasing in the stratosphere.
418 Whereas future increases in CH₄ are projected to lead to an increase in TCO at mid-latitudes
419 (Fleming *et al.*, 2011; Revell *et al.*, 2012), future increases in N₂O are projected to lead to a
420 decrease in TCO (Ravishankara, Daniel and Portmann, 2009; Eyring *et al.*, 2013). Unraveling
421 the impacts of CH₄ and N₂O on ozone is particularly complicated due to non-linear aspects of
422 stratospheric chemistry (Isaksen *et al.*, 2014; Revell *et al.*, 2015).

423 The continued recovery of the ozone layer (Oman *et al.*, 2010; Dhomse *et al.*, 2018;
424 Keeble *et al.*, 2021) faces a number of other threats. First, there is renewed interest in
425 commercial supersonic transport aircraft with the potential for substantial impacts on
426 stratospheric composition, including reductions in O₃, especially in the tropics, and increases
427 in stratospheric H₂O and black carbon aerosols, which together are estimated to result in a
428 warming of Earth's surface (Zhang *et al.*, 2023). Second, an expected order-of-magnitude
429 increase in space debris in the stratosphere from the burn-up of satellites and rocket stages
430 during reentry will increase the metallic content of stratospheric aerosols (Murphy *et al.*,
431 2023) and has the potential to cause ozone depletion (Ferreira *et al.*, 2024). In addition,
432 exhaust associated with an enormous future increase in the number of satellite launches
433 (58,000 launches by 2030, compared to 5,500 satellites in orbit as of spring 2022) (Howard
434 and Von Ah, 2022) could add black carbon to the stratosphere (Ross, Mills and Toohey,
435 2010), which could increase stratospheric temperatures, alter atmospheric circulation, and
436 cause a substantial reduction of TCO over NH mid-latitudes (Maloney *et al.*, 2022). The
437 current space-borne fleet of instruments provides an important observational baseline. During
438 the imminent data desert, future impacts on ozone of supersonic transport, rocket launches,
439 and vehicle reentry will be difficult to quantify.

440 Finally, tropospheric pollution from both industrial processes and biomass burning
441 can be injected into the stratosphere, including compounds such as CO, HCN, CH₃Cl,
442 CH₃CN, and CH₃OH measured by MLS and ACE-FTS (Bernath, 2006; Schwartz *et al.*,
443 2020). Analyses of MLS and ACE-FTS measurements have revealed that the summer
444 monsoon circulation in the upper troposphere/lower stratosphere that spans the region from
445 East Asia to the Middle East provides an efficient pathway for pollutants to enter the global
446 stratosphere (Li *et al.*, 2005; Fu *et al.*, 2006; Park *et al.*, 2007, 2008; Randel *et al.*, 2010).
447 Figure 9 shows the large perturbations in cloud ice water content (an indicator of the

448 occurrence of deep convection), CO, and CH₃Cl routinely observed by MLS that are
 449 associated with the Asian summer monsoon (Santee *et al.*, 2017). The CO and CH₃Cl
 450 enhancements are clearly related to pollutants emitted by industrial activities and biomass
 451 burning at the surface, based upon analyses of measurements from MLS and ACE-FTS as
 452 well as profiles of CO obtained by the space-borne Measurements Of Pollution In The
 453 Troposphere (MOPITT) instrument that extend into the lower troposphere (Jiang *et al.*, 2015;
 454 Smoydzin and Hoor, 2022). There are no plans in place to continue space-borne observations
 455 of tracers of tropospheric pollution, from which stratospheric injection is inferred. Again, the
 456 current suite of space-borne instruments provides an observational baseline and once MLS,
 457 ACE-FTS, and MOPITT cease operations, the future impact of pollution from industrial
 458 processes and biomass burning on the ozone layer will be difficult to directly characterize
 459 from observations.

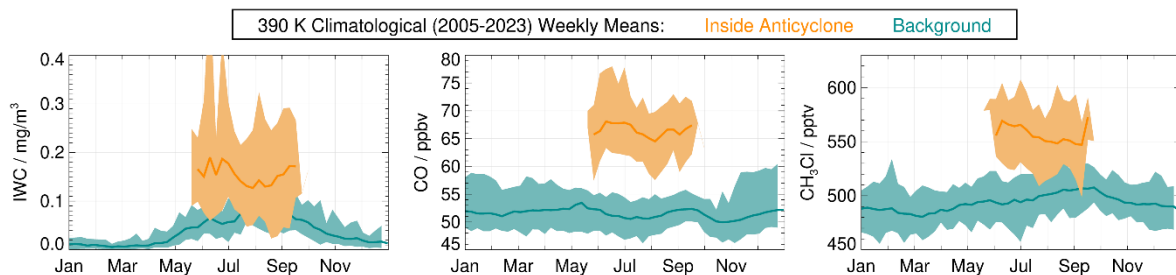


Figure 9. Weekly averages over the annual cycle of MLS measurements of cloud ice water content (IWC, a proxy for deep convection), CO, and CH₃Cl within the 15°N–45°N latitude band at 390 K potential temperature, which corresponds to ~15–17 km altitude in the region of the Asian monsoon during boreal summer. Dark orange lines represent climatological averages calculated over the period 2005–2023 within the anticyclonic monsoon circulation during the boreal summer season when it is defined; dark teal lines represent averages calculated over the latitude domain in the remaining portion of the hemisphere excluding the area of the Asian summer monsoon circulation. Paler shading represents the ranges of values measured over 2005–2023 in the respective regions. Update to Figure 3 of Santee *et al.* (2017).

460 **Polar Ozone.** Model simulations project that the size and depth of the Antarctic ozone hole
461 will decrease over the coming decades in a manner that largely follows future declines in the
462 abundance of stratospheric halogens (Oman *et al.*, 2010; Eyring *et al.*, 2013; Dhomse *et al.*,
463 2018; Keeble *et al.*, 2021). The size of the ozone hole varies from year to year, largely due to
464 meteorological influences, such as the rare SH sudden stratospheric warming that occurred in
465 2019 (Safieddine *et al.*, 2020; Wargan *et al.*, 2020; Bodeker and Kremser, 2021; Klekociuk *et*
466 *al.*, 2021), as well as exceptionally cold and long-lasting vortices in 2020 through 2023
467 (Grytsai *et al.*, 2022; Klekociuk *et al.*, 2022; Kramarova *et al.*, 2024). For O₃ and HCl at 52
468 hPa, MLS observed 4 σ and larger anomalies in 2019, 2020, and 2023 (Fig. 4).

469 Volcanic eruptions can increase the depth and size of the Antarctic ozone hole as the
470 ensuing enhancement in aerosol surface area facilitates chlorine activation (Hofmann and
471 Solomon, 1989). The April 2015 eruption of Calbuco in southern Chile led to the largest and
472 deepest ozone hole observed during the modern satellite era, primarily due to sulfate aerosol
473 that was transported into the Antarctic polar vortex (Solomon *et al.*, 2016; Stone *et al.*, 2017;
474 Zhu *et al.*, 2018). The deep ozone hole in 2021 has also been linked to the eruption of La
475 Soufriere (Yook, Thompson and Solomon, 2022).

476 The severity of polar ozone depletion exhibits much more interannual variability in the
477 Arctic compared to the Antarctic (Rex *et al.*, 2004, 2006; Tilmes *et al.*, 2004; Weber *et al.*,
478 2011; von der Gathen *et al.*, 2021) and is driven by the larger variability in NH
479 meteorological conditions. As stated in the Introduction, Arctic winter-spring periods with
480 long-lasting cold conditions exhibit severe chemical loss of ozone (Manney *et al.*, 2011,
481 2020; Griffin *et al.*, 2019; Lawrence *et al.*, 2020; Wohltmann *et al.*, 2020; Feng *et al.*, 2021;
482 Grooß and Müller, 2021). The increased variability of TCO in Arctic spring arises from year-
483 to-year differences in both dynamics and chemical loss due to anthropogenic halogens
484 (Hadjinicolaou and Pyle, 2004; Tegtmeier *et al.*, 2008; Calvo, Polvani and Solomon, 2015).
485 The large natural interannual variability of Arctic ozone has so far precluded the
486 identification of a statistically significant trend over the past two decades (WMO, 2022).

487 Analysis of seasonal declines in O₃ versus transport tracers such as N₂O and CH₄
488 constitutes an important tool for quantifying the impact of chemical loss on TCO, particularly
489 within the Arctic vortex (Salawitch *et al.*, 2002; Müller *et al.*, 2005; Tilmes *et al.*, 2006).
490 Profiles of N₂O provide an empirical measure of diabatic descent within the polar vortex,
491 which is necessary to distinguish dynamical and chemical impacts on O₃, especially in the

492 Arctic (Manney *et al.*, 2011, 2020; Feng *et al.*, 2021). Some studies suggest that particularly
493 cold Arctic winter-spring periods conducive to severe chemical ozone loss will become more
494 common in the future, as stratospheric temperatures decrease with climate change (Rex *et al.*,
495 2004, 2006; von der Gathen *et al.*, 2021). During the imminent data desert, space-borne
496 profiles of vertically resolved measurements of stratospheric halogens and transport tracers
497 will not be available. Space-borne profiles of O₃ will also not be available during the critical
498 period of vortex formation, which occurs during polar night. Therefore, diagnosis of the
499 causes of interannual variations in ozone within the Arctic and Antarctic polar vortices will
500 be forced to rely on simulated profiles of O₃. Most importantly, our ability to empirically
501 quantify the degree of chemical ozone loss in persistently cold winters in either hemisphere,
502 as well as the impact of future volcanic eruptions on chemical (Solomon *et al.*, 2016) and
503 dynamical (Ivy *et al.*, 2017) conditions in the polar regions, will be severely compromised.

504 **Surface Climate**

505 The long-term change in stratospheric water vapor has been shown to impact decadal trends
506 in the rate of global warming (Solomon *et al.*, 2010). Future increases in stratospheric H₂O
507 may constitute an important climate feedback that might be the same order of magnitude as
508 feedbacks involving surface albedo and tropospheric clouds (Banerjee *et al.*, 2019; Tao *et al.*,
509 2023). These analyses rely on homogenized, long-term records of stratospheric H₂O from a
510 series of limb-profiling satellite instruments, which currently utilize measurements from MLS
511 as the primary daily near-global source of data (Froidevaux *et al.*, 2015; Davis *et al.*, 2016).
512 The accurate quantification of future climate change on decadal and centennial timescales is a
513 coupled chemistry-climate problem that requires continuous measurements of stratospheric
514 profiles of ozone, water vapor, and aerosols (IPCC, 2021).

515 Volcanic eruptions that inject sulfate aerosols into the stratosphere can also impact
516 climate, not only on annual timescales but also on decadal timescales, depending upon the
517 sequence of eruptions (Solomon *et al.*, 2011; Marshall *et al.*, 2022). The eruption of Mount
518 Pinatubo injected nearly 20 Tg of SO₂ into the stratosphere (Bluth *et al.*, 1992), which led to
519 a reduction in global mean surface temperature (GMST) between about 0.1 and 0.4°C (Santer
520 *et al.*, 2001; Thompson *et al.*, 2009; Canty *et al.*, 2013; Fujiwara, Martineau and Wright,
521 2020). In contrast, the Hunga eruption injected between 0.5 and 0.7 Tg of SO₂ into the
522 stratosphere (Carn *et al.*, 2022; Sellitto *et al.*, 2022; Duchamp *et al.*, 2023) and is estimated to

523 have resulted in a cooling of less than about 0.04°C of Earth’s surface in the SH in 2022
524 (Schoeberl *et al.*, 2023). This small net cooling occurred because the attenuation of solar
525 radiation by aerosols was partly cancelled by heating due to the large increase in stratospheric
526 water vapor. Without observations of stratospheric water vapor and aerosols from MLS,
527 SAGE III/ISS, and OMPS-LP, it would have been difficult to diagnose the climate impact of
528 Hunga.

529 **Geo-Engineering for Climate Change Mitigation**

530 There is increasing dialogue regarding the possibility of using stratospheric aerosol injection
531 (SAI) as a means to slow the rate of global warming, as noted in reports on SAI by the U.S.
532 National Academy of Sciences in 2015 (NAS, 2015) and 2021 (NAS, 2021), as well as a
533 chapter on this topic in the most recent Scientific Assessment of Ozone Depletion report
534 (Haywood *et al.*, 2022). It is nearly inconceivable that the world is facing an imminent data
535 desert with respect to monitoring stratospheric composition and the recovery of the ozone
536 layer, even as discussions around the possibility of geo-engineering the climate by SAI are
537 ongoing (Tilmes *et al.*, 2024).

538 The actual response of stratospheric ozone to injection of sulfate or other types of
539 aerosols depends on details of the chemical and dynamical effects of such an action
540 (Haywood *et al.*, 2022). Injection of sulfate aerosols into the stratosphere has the potential to
541 delay the recovery of the ozone layer from depletion by anthropogenic halogens in the polar
542 regions of both hemispheres (Tilmes, Müller and Salawitch, 2008; Pitari *et al.*, 2014; Lee *et*
543 *al.*, 2021) as well as over the rest of the global stratosphere (Heckendorn *et al.*, 2009; Tilmes
544 *et al.*, 2012; Robrecht *et al.*, 2021). The 2006 paper that invigorated debate among the
545 world’s scientists and policy makers about climate intervention used the response of TCO
546 and GMST to the 1991 eruption of Mount Pinatubo as an analogy for the effects of SAI
547 (Crutzen, 2006). Figure 10 shows the response of the GMST anomaly to the 1991 eruption of
548 Mount Pinatubo and the earlier eruption of El Chichón, as well as the TCO anomaly between
549 60°S and 60°N found using a standard regression method. While stratospheric halogen
550 loading is now somewhat lower than at the time of the El Chichón and Mount Pinatubo
551 eruptions, if SAI were to be used for “peak shaving” of global temperature (Haywood *et al.*,
552 2022) in the near future, anthropogenic chlorine would still be much higher than at the time
553 of the onset of the Antarctic ozone hole, and chlorine-catalyzed ozone loss would therefore

554 be expected. Regardless, the ozone decreases that followed these eruptions, which are
555 straightforward to quantify in the TCO data record, serve as an important starting point for
556 discussion of the consequences of deliberate SAI. Were SAI to be implemented at a
557 magnitude that rivals the stratospheric injection of sulfur following the eruption of Mount
558 Pinatubo, the data shown in Fig. 10 suggest that ozone depletion could occur over densely
559 populated regions of the globe. Should SAI be undertaken while we are in the midst of the
560 data desert, our ability to assess the chemical and dynamical response of the stratosphere to
561 such climate intervention efforts will be severely limited.

562

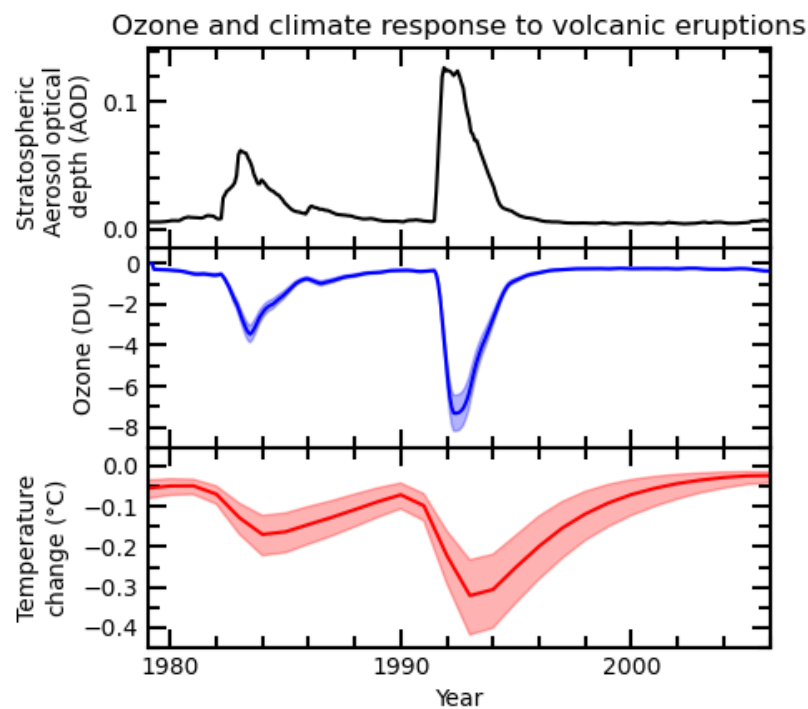


Figure 10. Time series of stratospheric aerosol optical depth (SAOD), the anomaly in TCO (ΔO_3) between 60°S and 60°N, and the anomaly in global mean surface temperature (ΔT) following the volcanic eruptions of El Chichón and Mount Pinatubo in 1982 and 1991, respectively. The monthly SAOD time series is based on integration of extinction coefficients from the GloSSAC v2 database (Thomason *et al.*, 2018; Kovilakam *et al.*, 2023). The ΔO_3 time series is the computed impact of SAOD on ΔO_3 found for a multiple linear regression of monthly TCO averaged over 60°S to 60°N versus the following terms: equivalent effective stratospheric chlorine for 3 yr old air, total solar irradiance, SAOD, the QBO in the zonal mean wind in the tropical lower stratosphere, and the El Niño Southern Oscillation, as in Figure 3-1 of Chipperfield *et al.*, 2007. The ΔO_3 time series is smoothed with a 6-month running mean; the shaded region defines the 2σ uncertainty based on a conditional regression. The time series of ΔT and the 2σ uncertainties represented by the shaded region are obtained from the model output used to construct Figure 7.8 of the IPCC Sixth Assessment Report (IPCC, 2021).

563 **Concluding Thoughts**

564 The stratosphere is not a solved problem. The past few years have marked an era of discovery
565 and new understanding, greatly enabled by the portfolio of observations from the ACE-FTS
566 and MLS instruments. The atmospheric science community now faces an impending “data
567 desert” as ACE-FTS is over 20 years old and MLS nears the end of its operational lifetime.
568 This data gap will occur at a time when the recovery of stratospheric ozone at NH
569 midlatitudes has stalled and just after the impacts on stratospheric ozone of wildfires and an
570 undersea volcanic eruption have been quantified for the first time. Future impacts to the
571 recovery of the ozone layer from a wide range of tropospheric pollutants, changes in the
572 strength of the BDC in response to increasing GHGs, the possibility of cold Arctic winters
573 getting colder, the emerging threats posed by the potential for increasing extreme wildfires
574 and space debris, as well as the specter of geo-engineering for climate change mitigation
575 through SAI will be difficult to quantify in the absence of the types of observations provided
576 by ACE-FTS and MLS. Similarly, our ability to understand future changes to stratospheric
577 water vapor and its attendant chemical and climate impacts will be diminished. Routes to
578 ensuring long-term continuity for these measurements are unclear. Upon loss of the
579 measurement capability provided by these instruments, our ability to understand the evolution
580 of stratospheric ozone and water vapor and the wide-reaching impacts on human health and
581 the Earth’s climate system will be severely hindered. While specific details of future
582 measurement requirements are beyond the scope of this publication, we suggest that the
583 atmospheric science community begin formally developing requirements for future space-
584 borne observations of stratospheric composition. Such requirements should target: (i)
585 continuous measurement of long-term trends in stratospheric composition focused on the
586 “health” of the ozone layer, (ii) interactions between the ozone layer and Earth’s climate
587 system, and (iii) unexpected events that could cause significant departures from predicted
588 behavior such as a particularly severe ozone hole, or reductions in total column ozone over
589 broad latitudinal regions due to wildfires or volcanoes. Finally, the future observing system
590 should be capable of monitoring solar radiation management by SAI, including the
591 identification of the geographic origin and chemical nature of any possible future
592 unannounced enhancement of the stratospheric aerosol layer to mitigate global warming.

593 *Acknowledgments*

594 We thank the three reviewers for their thorough, constructive reviews that led to an
595 improved manuscript. We also thank Daniele Minganti for sharing thoughts on the cause of
596 the dynamically driven anomalies of O₃, HCl, and N₂O that occurred in 2019. RJS and LAM
597 were supported by the NASA Atmospheric Composition Modeling and Analysis Program
598 under grant 80NSSC19K098. JBS was supported by the NASA DCOTSS program under
599 grant 80NSSC19K0326. HS was supported by NASA's NRESS-II contract with Agile
600 Decision Sciences. KW was supported by NASA's Modeling, Analysis and Prediction
601 program. MRS was supported by NASA grant 80NSSC21K1965. MPC and RH were
602 supported by the NERC LSO3 project (NE/V011863/1); MPC was also supported by ESA
603 (OREGANO 4000137112/22/I-AG). SS and KS were supported by NSF grant 2316980. The
604 NSF National Center for Atmospheric Research is sponsored by the U.S. National Science
605 Foundation, and work at the Jet Propulsion Laboratory, California Institute of Technology is
606 carried out under a contract with the National Aeronautics and Space Administration
607 (80NM0018D0004). The SCISAT-1 satellite, along with ACE-FTS and MAESTRO
608 instruments and data production, are supported by the Canadian Space Agency.

609 *Data Availability Statement*

610 Data from Aura MLS are available at
611 <https://disc.gsfc.nasa.gov/datasets?page=1&keywords=AURA%20MLS>, data from SCISAT-
612 1 ACE-FTS are available at https://borealisdata.ca/dataverse/ace-fts_data_quality. Output
613 from M2-SCREAM is at [https://disc.gsfc.nasa.gov/datasets?keywords=M2-
614 SCREAM&page=1](https://disc.gsfc.nasa.gov/datasets?keywords=M2-SCREAM&page=1) and the GloSSAC climatology of stratospheric aerosol properties is at
615 <https://asdc.larc.nasa.gov/project/GloSSAC>. Finally, the volcanically induced temperature
616 anomaly shown in figure 10 was obtained from
617 https://data.ceda.ac.uk/badc/ar6_wg1/data/ch_07/ch7_fig08/v20220721.

- 619 Abalos, M. *et al.* (2021) ‘The Brewer–Dobson circulation in CMIP6’, *Atmos. Chem. Phys.*,
620 21(17), pp. 13571–13591. Available at: <https://doi.org/10.5194/acp-21-13571-2021>.
- 621 An, M. *et al.* (2021) ‘Rapid increase in dichloromethane emissions from China inferred
622 through atmospheric observations’, *Nature Communications*, 12(1), p. 7279. Available at:
623 <https://doi.org/10.1038/s41467-021-27592-y>.
- 624 Anderson, J.G. and Clapp, C.E. (2018) ‘Coupling free radical catalysis, climate change, and
625 human health’, *Physical chemistry chemical physics*, 20(16), pp. 10569–10587.
- 626 Asher, E. *et al.* (2023) ‘Unexpectedly rapid aerosol formation in the Hunga Tonga plume’,
627 *Proceedings of the National Academy of Sciences*, 120(46), p. e2219547120. Available
628 at: <https://doi.org/10.1073/pnas.2219547120>.
- 629 Bais, A.F. *et al.* (2018) ‘Environmental effects of ozone depletion, UV radiation and
630 interactions with climate change: UNEP Environmental Effects Assessment Panel, update
631 2017’, *Photochemical & Photobiological Sciences*, 17(2), pp. 127–179. Available at:
632 <https://doi.org/10.1039/c7pp90043k>.
- 633 Baldwin, M.P. *et al.* (2021) ‘Sudden Stratospheric Warmings’, *Reviews of Geophysics*, 59(1),
634 p. e2020RG000708. Available at: <https://doi.org/10.1029/2020RG000708>.
- 635 Ball, W.T. *et al.* (2018) ‘Evidence for a continuous decline in lower stratospheric ozone
636 offsetting ozone layer recovery’, *Atmos. Chem. Phys.*, 18(2), pp. 1379–1394. Available
637 at: <https://doi.org/10.5194/acp-18-1379-2018>.
- 638 Ball, W.T. *et al.* (2020) ‘Inconsistencies between chemistry–climate models and observed
639 lower stratospheric ozone trends since 1998’, *Atmos. Chem. Phys.*, 20(16), pp. 9737–
640 9752. Available at: <https://doi.org/10.5194/acp-20-9737-2020>.
- 641 Banerjee, A. *et al.* (2019) ‘Stratospheric water vapor: an important climate feedback’,
642 *Climate Dynamics*, 53(3), pp. 1697–1710. Available at: <https://doi.org/10.1007/s00382-019-04721-4>.
- 643
- 644 Bednarz, E.M. *et al.* (2022) ‘Atmospheric impacts of chlorinated very short-lived substances
645 over the recent past – Part 1: Stratospheric chlorine budget and the role of transport’,
646 *Atmos. Chem. Phys.*, 22(16), pp. 10657–10676. Available at: <https://doi.org/10.5194/acp-22-10657-2022>.
- 647
- 648 Bednarz, E.M. *et al.* (2023) ‘Injection strategy – a driver of atmospheric circulation and
649 ozone response to stratospheric aerosol geoengineering’, *Atmos. Chem. Phys.*, 23(21), pp.
650 13665–13684. Available at: <https://doi.org/10.5194/acp-23-13665-2023>.
- 651 Bednarz, E.M., Hossaini, R. and Chipperfield, M.P. (2023) ‘Atmospheric impacts of
652 chlorinated very short-lived substances over the recent past – Part 2: Impacts on ozone’,
653 *Atmos. Chem. Phys.*, 23(21), pp. 13701–13711. Available at: <https://doi.org/10.5194/acp-23-13701-2023>.
- 654
- 655 Bernath, P., Boone, C. and Crouse, J. (2022) ‘Wildfire smoke destroys stratospheric ozone’,
656 *Science*, 375(6586), pp. 1292–1295. Available at:
657 <https://doi.org/10.1126/science.abm5611>.
- 658 Bernath, P. and Fernando, A.M. (2018) ‘Trends in stratospheric HCl from the ACE satellite
659 mission’, *Journal of Quantitative Spectroscopy and Radiative Transfer*, 217, pp. 126–
660 129. Available at: <https://doi.org/10.1016/j.jqsrt.2018.05.027>.
- 661 Bernath, P.F. *et al.* (2005) ‘Atmospheric Chemistry Experiment (ACE): Mission overview’,
662 *Geophysical Research Letters*, 32(15). Available at:
663 <https://doi.org/10.1029/2005GL022386>.
- 664 Bernath, P.F. (2006) ‘Atmospheric chemistry experiment (ACE): Analytical chemistry from
665 orbit’, *TrAC Trends in Analytical Chemistry*, 25(7), pp. 647–654. Available at:

666 <https://doi.org/10.1016/j.trac.2006.05.001>.

667 Bluth, G.J.S. *et al.* (1992) ‘Global tracking of the SO₂ clouds from the June, 1991 Mount
668 Pinatubo eruptions’, *Geophysical Research Letters*, 19(2), pp. 151–154. Available at:
669 <https://doi.org/10.1029/91GL02792>.

670 Bodeker, G.E. and Kremser, S. (2021) ‘Indicators of Antarctic ozone depletion: 1979 to
671 2019’, *Atmos. Chem. Phys.*, 21(7), pp. 5289–5300. Available at:
672 <https://doi.org/10.5194/acp-21-5289-2021>.

673 Butchart, N. *et al.* (2006) ‘Simulations of anthropogenic change in the strength of the
674 Brewer–Dobson circulation’, *Climate Dynamics*, 27(7), pp. 727–741. Available at:
675 <https://doi.org/10.1007/s00382-006-0162-4>.

676 Butchart, N. *et al.* (2011) ‘Multimodel climate and variability of the stratosphere’, *Journal of*
677 *Geophysical Research: Atmospheres*, 116(D5). Available at:
678 <https://doi.org/10.1029/2010JD014995>.

679 Calvo, N., Polvani, L.M. and Solomon, S. (2015) ‘On the surface impact of Arctic
680 stratospheric ozone extremes’, *Environmental Research Letters*, 10(9), p. 94003.
681 Available at: <https://doi.org/10.1088/1748-9326/10/9/094003>.

682 Canty, T. *et al.* (2013) ‘An empirical model of global climate – Part 1: A critical evaluation
683 of volcanic cooling’, *Atmos. Chem. Phys.*, 13(8), pp. 3997–4031. Available at:
684 <https://doi.org/10.5194/acp-13-3997-2013>.

685 Carn, S.A. *et al.* (2022) ‘Out of the blue: Volcanic SO₂ emissions during the 2021–2022
686 eruptions of Hunga Tonga—Hunga Ha’apai (Tonga)’, *Frontiers in Earth Science*, 10.
687 Available at: [https://www.frontiersin.org/journals/earth-](https://www.frontiersin.org/journals/earth-science/articles/10.3389/feart.2022.976962)
688 [science/articles/10.3389/feart.2022.976962](https://www.frontiersin.org/journals/earth-science/articles/10.3389/feart.2022.976962).

689 Chipperfield, M.P. and Bekki, S. (2024) ‘Opinion: Stratospheric ozone – depletion, recovery
690 and new challenges’, *Atmos. Chem. Phys.*, 24(4), pp. 2783–2802. Available at:
691 <https://doi.org/10.5194/acp-24-2783-2024>.

692 Chipperfield, M.P. *et al.* (2007) Global Ozone: Past and Present, Chapter 3 in Scientific
693 Assessment of Ozone Depletion: 2006, Global Ozone Research and Monitoring Project -
694 Report No. 50, 572 pp., World Meteorological Organization. Geneva, Switzerland.

695 Chipperfield, M.P. *et al.* (2018) ‘On the cause of recent variations in lower stratospheric
696 ozone’, *Geophysical Research Letters*, 45(11), pp. 5718–5726. Available at:
697 <https://doi.org/10.1029/2018GL078071>.

698 Chipperfield, M.P. *et al.* (2020) ‘Renewed and emerging concerns over the production and
699 emission of ozone-depleting substances’, *Nature Reviews Earth & Environment*, 1(5), pp.
700 251–263. Available at: <https://doi.org/10.1038/s43017-020-0048-8>.

701 Chouza, F. *et al.* (2020) ‘Long-term (1999–2019) variability of stratospheric aerosol over
702 Mauna Loa, Hawaii, as seen by two co-located lidars and satellite measurements’, *Atmos.*
703 *Chem. Phys.*, 20(11), pp. 6821–6839. Available at: [https://doi.org/10.5194/acp-20-6821-](https://doi.org/10.5194/acp-20-6821-2020)
704 [2020](https://doi.org/10.5194/acp-20-6821-2020).

705 Coldewey-Egbers, M. *et al.* (2020) ‘Comparison of GTO-ECV and adjusted MERRA-2 total
706 ozone columns from the last 2 decades and assessment of interannual variability’, *Atmos.*
707 *Meas. Tech.*, 13(3), pp. 1633–1654. Available at: [https://doi.org/10.5194/amt-13-1633-](https://doi.org/10.5194/amt-13-1633-2020)
708 [2020](https://doi.org/10.5194/amt-13-1633-2020).

709 Connor, B.J. *et al.* (2013) ‘Re-analysis of ground-based microwave ClO measurements from
710 Mauna Kea, 1992 to early 2012’, *Atmos. Chem. Phys.*, 13(17), pp. 8643–8650. Available
711 at: <https://doi.org/10.5194/acp-13-8643-2013>.

712 Coy, L. *et al.* (2022) ‘Stratospheric Circulation Changes Associated With the Hunga Tonga-
713 Hunga Ha’apai Eruption’, *Geophysical Research Letters*, 49(22), p. e2022GL100982.
714 Available at: <https://doi.org/10.1029/2022GL100982>.

715 Crutzen, P.J. (2006) ‘Albedo Enhancement by Stratospheric Sulfur Injections: A Contribution
716 to Resolve a Policy Dilemma?’, *Climatic Change*, 77(3–4), pp. 211–219. Available at:
717 <https://doi.org/10.1007/s10584-006-9101-y>.

718 Davis, S.M. *et al.* (2016) ‘The Stratospheric Water and Ozone Satellite Homogenized
719 (SWOOSH) database: a long-term database for climate studies’, *Earth Syst. Sci. Data*,
720 8(2), pp. 461–490. Available at: <https://doi.org/10.5194/essd-8-461-2016>.

721 Davis, S.M. *et al.* (2021) ‘Validation of SAGE III/ISS Solar Water Vapor Data With
722 Correlative Satellite and Balloon-Borne Measurements’, *Journal of Geophysical
723 Research: Atmospheres*, 126(2), p. e2020JD033803. Available at:
724 <https://doi.org/10.1029/2020JD033803>.

725 De Mazière, M. *et al.* (2018) ‘The Network for the Detection of Atmospheric Composition
726 Change (NDACC): history, status and perspectives’, *Atmos. Chem. Phys.*, 18(7), pp.
727 4935–4964. Available at: <https://doi.org/10.5194/acp-18-4935-2018>.

728 Dessler, A.E. *et al.* (2013) ‘Stratospheric water vapor feedback’, *Proceedings of the National
729 Academy of Sciences*, 110(45), pp. 18087–18091. Available at:
730 <https://doi.org/10.1073/pnas.1310344110>.

731 Dhomse, S.S. *et al.* (2018) ‘Estimates of ozone return dates from Chemistry-Climate Model
732 Initiative simulations’, *Atmos. Chem. Phys.*, 18(11), pp. 8409–8438. Available at:
733 <https://doi.org/10.5194/acp-18-8409-2018>.

734 Di Virgilio, G. *et al.* (2019) ‘Climate Change Increases the Potential for Extreme Wildfires’,
735 *Geophysical Research Letters*, 46(14), pp. 8517–8526. Available at:
736 <https://doi.org/10.1029/2019GL083699>.

737 Duchamp, C. *et al.* (2023) ‘Observation of the Aerosol Plume From the 2022 Hunga Tonga—
738 Hunga Ha’apai Eruption With SAGE III/ISS’, *Geophysical Research Letters*, 50(18), p.
739 e2023GL105076. Available at: <https://doi.org/10.1029/2023GL105076>.

740 Dvortsov, V.L. and Solomon, S. (2001) ‘Response of the stratospheric temperatures and
741 ozone to past and future increases in stratospheric humidity’, *Journal of Geophysical
742 Research: Atmospheres*, 106(D7), pp. 7505–7514. Available at:
743 <https://doi.org/10.1029/2000JD900637>.

744 Evan, S. *et al.* (2024) ‘Rapid ozone depletion after humidification of the stratosphere by the
745 Hunga Tonga Eruption’, *Science*, 382(6668), p. eadg2551. Available at:
746 <https://doi.org/10.1126/science.adg2551>.

747 Eyring, V. *et al.* (2013) ‘Long-term ozone changes and associated climate impacts in CMIP5
748 simulations’, *Journal of Geophysical Research: Atmospheres*, 118(10), pp. 5029–5060.
749 Available at: <https://doi.org/10.1002/jgrd.50316>.

750 Fahey, D.W. *et al.* (1993) ‘In situ measurements constraining the role of sulphate aerosols in
751 mid-latitude ozone depletion’, *Nature*, 363(6429), pp. 509–514. Available at:
752 <https://doi.org/10.1038/363509a0>.

753 Fang, X. *et al.* (2019) ‘Rapid increase in ozone-depleting chloroform emissions from China’,
754 *Nature Geoscience*, 12(2), pp. 89–93. Available at: <https://doi.org/10.1038/s41561-018-0278-2>.

755

756 Feng, W. *et al.* (2021) ‘Arctic Ozone Depletion in 2019/20: Roles of Chemistry, Dynamics
757 and the Montreal Protocol’, *Geophysical Research Letters*, 48(4), p. e2020GL091911.
758 Available at: <https://doi.org/10.1029/2020GL091911>.

759 Ferreira, J.P. *et al.* (2024) ‘Potential Ozone Depletion From Satellite Demise During
760 Atmospheric Reentry in the Era of Mega-Constellations’, *Geophysical Research Letters*,
761 51(11), p. e2024GL109280. Available at: <https://doi.org/10.1029/2024GL109280>.

762 Fleming, E.L. *et al.* (2011) ‘A model study of the impact of source gas changes on the
763 stratosphere for 1850–2100’, *Atmos. Chem. Phys.*, 11(16), pp. 8515–8541. Available at:

764 <https://doi.org/10.5194/acp-11-8515-2011>.

765 Fleming, E.L. *et al.* (2024) ‘Stratospheric Temperature and Ozone Impacts of the Hunga

766 Tonga-Hunga Ha’apai Water Vapor Injection’, *Journal of Geophysical Research:*

767 *Atmospheres*, 129(1), p. e2023JD039298. Available at:

768 <https://doi.org/10.1029/2023JD039298>.

769 Flury, T., Wu, D.L. and Read, W.G. (2013) ‘Variability in the speed of the Brewer–Dobson

770 circulation as observed by Aura/MLS’, *Atmos. Chem. Phys.*, 13(9), pp. 4563–4575.

771 Available at: <https://doi.org/10.5194/acp-13-4563-2013>.

772 Froidevaux, L. *et al.* (2006) ‘Temporal decrease in upper atmospheric chlorine’, *Geophysical*

773 *Research Letters*, 33(23). Available at: <https://doi.org/10.1029/2006GL027600>.

774 Froidevaux, L. *et al.* (2015) ‘Global Ozone Chemistry And Related trace gas Data records

775 for the Stratosphere (GOZCARDS): methodology and sample results with a focus on

776 HCl, H₂O, and O₃’, *Atmos. Chem. Phys.*, 15(18), pp. 10471–10507. Available at:

777 <https://doi.org/10.5194/acp-15-10471-2015>.

778 Froidevaux, L. *et al.* (2022) ‘Upper stratospheric ClO and HOCl trends (2005–2020): Aura

779 Microwave Limb Sounder and model results’, *Atmos. Chem. Phys.*, 22(7), pp. 4779–

780 4799. Available at: <https://doi.org/10.5194/acp-22-4779-2022>.

781 Fu, R. *et al.* (2006) ‘Short circuit of water vapor and polluted air to the global stratosphere by

782 convective transport over the Tibetan Plateau’, *Proceedings of the National Academy of*

783 *Sciences*, 103(15), pp. 5664–5669. Available at:

784 <https://doi.org/10.1073/pnas.0601584103>.

785 Fujiwara, M., Martineau, P. and Wright, J.S. (2020) ‘Surface temperature response to the

786 major volcanic eruptions in multiple reanalysis data sets’, *Atmos. Chem. Phys.*, 20(1), pp.

787 345–374. Available at: <https://doi.org/10.5194/acp-20-345-2020>.

788 Garcia, R.R. and Randel, W.J. (2008) ‘Acceleration of the Brewer–Dobson Circulation due to

789 Increases in Greenhouse Gases’, *Journal of the Atmospheric Sciences*, 65(8), pp. 2731–

790 2739. Available at: <https://doi.org/10.1175/2008JAS2712.1>.

791 Griffin, D. *et al.* (2019) ‘Stratospheric ozone loss in the Arctic winters between 2005 and

792 2013 derived with ACE-FTS measurements’, *Atmos. Chem. Phys.*, 19(1), pp. 577–601.

793 Available at: <https://doi.org/10.5194/acp-19-577-2019>.

794 Groß, J.U. and Müller, R. (2021) ‘Simulation of Record Arctic Stratospheric Ozone

795 Depletion in 2020’, *Journal of Geophysical Research: Atmospheres*, 126(12). Available

796 at: <https://doi.org/10.1029/2020JD033339>.

797 Grytsai, A. *et al.* (2022) ‘Antarctic planetary wave spectrum under different polar vortex

798 conditions in 2019 and 2020 based on total ozone column data’, *Ukrainian Antarctic*

799 *Journal*, 20(1(24) SE-Articles). Available at: [https://doi.org/10.33275/1727-](https://doi.org/10.33275/1727-7485.1.2022.687)

800 [7485.1.2022.687](https://doi.org/10.33275/1727-7485.1.2022.687).

801 Hadjinicolaou, P. and Pyle, J.A. (2004) ‘The Impact of Arctic Ozone Depletion on Northern

802 Middle Latitudes: Interannual Variability and Dynamical Control’, *Journal of*

803 *Atmospheric Chemistry*, 47(1), pp. 25–43. Available at:

804 <https://doi.org/10.1023/B:JOCH.0000012242.06578.6c>.

805 Haywood, J. *et al.* (2022) *Stratospheric Aerosol Injection and its Potential Effect on the*

806 *Stratospheric Ozone Layer, Chapter 6 in Scientific Assessment of Ozone Depletion: 2022,*

807 *GAW Report No. 278, WMO, Geneva, Switzerland.* Geneva, Switzerland, 509 pp.

808 Heckendorn, P. *et al.* (2009) ‘The impact of geoengineering aerosols on stratospheric

809 temperature and ozone’, *Environmental Research Letters*, 4(4), p. 45108. Available at:

810 <https://doi.org/10.1088/1748-9326/4/4/045108>.

811 Hegglin, M.I. *et al.* (2014) ‘Vertical structure of stratospheric water vapour trends derived

812 from merged satellite data’, *Nature Geoscience*, 7(10), pp. 768–776. Available at:

813 <https://doi.org/10.1038/ngeo2236>.

814 Hofmann, D.J. and Solomon, S. (1989) ‘Ozone destruction through heterogeneous chemistry
815 following the eruption of El Chichón’, *Journal of Geophysical Research: Atmospheres*,
816 94(D4), pp. 5029–5041. Available at: <https://doi.org/10.1029/JD094iD04p05029>.

817 Holden, Z.A. *et al.* (2018) ‘Decreasing fire season precipitation increased recent western US
818 forest wildfire activity’, *Proceedings of the National Academy of Sciences*, 115(36), pp.
819 E8349–E8357. Available at: <https://doi.org/10.1073/pnas.1802316115>.

820 Hossaini, R. *et al.* (2017) ‘The increasing threat to stratospheric ozone from
821 dichloromethane’, *Nature Communications*, 8, pp. 1–9. Available at:
822 <https://doi.org/10.1038/ncomms15962>.

823 Hossaini, R. *et al.* (2019) ‘Recent trends in stratospheric chlorine from very short-lived
824 substances’, *Journal of Geophysical Research: Atmospheres*, 124(4), pp. 2318–2335.
825 Available at: <https://doi.org/10.1029/2018JD029400>.

826 Hossaini, R. *et al.* (2024) ‘On the atmospheric budget of ethylene dichloride and its impact on
827 stratospheric chlorine and ozone (2002-2020)’, *Atmos. Chem. Phys.*, 24, 13457–13475,
828 <https://doi.org/10.5194/acp-24-13457-2024>.

829 Howard, K. and Von Ah, A. (2022) ‘Large Constellations of Satellites: Mitigating
830 Environmental and Other Effects’, *Government Accountability Office, Washington, DC,*
831 *USA, GAO Report No. GAO-22-105166* [Preprint].

832 Hu, S. and Vallis, G.K. (2019) ‘Meridional structure and future changes of tropopause height
833 and temperature’, *Quarterly Journal of the Royal Meteorological Society*, 145(723), pp.
834 2698–2717. Available at: <https://doi.org/10.1002/qj.3587>.

835 Hurst, D.F. *et al.* (2011) ‘Stratospheric water vapor trends over Boulder, Colorado: Analysis
836 of the 30 year Boulder record’, *Journal of Geophysical Research: Atmospheres*, 116(D2).
837 Available at: <https://doi.org/10.1029/2010JD015065>.

838 Illingworth, A.J. *et al.* (2015) ‘The EarthCARE satellite: the next step forward in global
839 measurements of clouds, aerosols, precipitation, and radiation’, *Bulletin of the American*
840 *Meteorological Society*, 96(8), pp. 1311–1332. Available at:
841 <https://doi.org/10.1175/BAMS-D-12-00227.1>.

842 IPCC (2021) ‘Index’, in V. Masson-Delmotte *et al.* (eds) *Climate Change 2021: The Physical*
843 *Science Basis. Contribution of Working Group I to the Sixth Assessment Report of the*
844 *Intergovernmental Panel on Climate Change*. Cambridge, United Kingdom and New
845 York, NY, USA: Cambridge University Press, p. In press.

846 Isaksen, I.S.A. *et al.* (2014) ‘Atmospheric Ozone and Methane in a Changing Climate’,
847 *Atmosphere*, pp. 518–535. Available at: <https://doi.org/10.3390/atmos5030518>.

848 Ivy, D.J. *et al.* (2017) ‘The influence of the Calbuco eruption on the 2015 Antarctic ozone
849 hole in a fully coupled chemistry-climate model’, *Geophysical Research Letters*, 44(5),
850 pp. 2556–2561. Available at: <https://doi.org/10.1002/2016GL071925>.

851 Jaross, G. *et al.* (2014) ‘OMPS Limb Profiler instrument performance assessment’, *Journal of*
852 *Geophysical Research: Atmospheres*, 119(7), pp. 4399–4412. Available at:
853 <https://doi.org/10.1002/2013JD020482>.

854 Jiang, Z. *et al.* (2015) ‘Sensitivity of top-down CO source estimates to the modeled vertical
855 structure in atmospheric CO’, *Atmos. Chem. Phys.*, 15(3), pp. 1521–1537. Available at:
856 <https://doi.org/10.5194/acp-15-1521-2015>.

857 Kablick III, G.P. *et al.* (2020) ‘Australian PyroCb Smoke Generates Synoptic-Scale
858 Stratospheric Anticyclones’, *Geophysical Research Letters*, 47(13), p. e2020GL088101.
859 Available at: <https://doi.org/10.1029/2020GL088101>.

860 Keeble, J. *et al.* (2021) ‘Evaluating stratospheric ozone and water vapour changes in CMIP6
861 models from 1850 to 2100’, *Atmospheric Chemistry and Physics*, 21(6), pp. 5015–5061.

862 Available at: <https://doi.org/10.5194/acp-21-5015-2021>.

863 Khaykin, S. *et al.* (2020) ‘The 2019/20 Australian wildfires generated a persistent smoke-
864 charged vortex rising up to 35 km altitude’, *Communications Earth & Environment*, 1(1),
865 p. 22. Available at: <https://doi.org/10.1038/s43247-020-00022-5>.

866 Khaykin, S. *et al.* (2022) ‘Global perturbation of stratospheric water and aerosol burden by
867 Hunga eruption’, *Communications Earth & Environment*, 3(1), p. 316. Available at:
868 <https://doi.org/10.1038/s43247-022-00652-x>.

869 Kirk-Davidoff, D.B. *et al.* (1999) ‘The effect of climate change on ozone depletion through
870 changes in stratospheric water vapour’, *Nature*, 402(6760), pp. 399–401. Available at:
871 <https://doi.org/10.1038/46521>.

872 Klekociuk, A.R. *et al.* (2021) ‘The Antarctic ozone hole during 2018 and 2019’, *Journal of*
873 *Southern Hemisphere Earth Systems Science*, 71(1), pp. 66–91. Available at:
874 <https://doi.org/10.1071/ES20010>.

875 Klekociuk, A.R. *et al.* (2022) ‘The Antarctic ozone hole during 2020’, *Journal of Southern*
876 *Hemisphere Earth Systems Science*, 72(1), pp. 19–37. Available at:
877 <https://doi.org/10.1071/ES21015>.

878 Kloss, C. *et al.* (2022) ‘Aerosol Characterization of the Stratospheric Plume From the
879 Volcanic Eruption at Hunga Tonga 15 January 2022’, *Geophysical Research Letters*,
880 49(16), p. e2022GL099394. Available at: <https://doi.org/10.1029/2022GL099394>.

881 Knepp, T.N. *et al.* (2024) ‘Characterization of stratospheric particle size distribution
882 uncertainties using SAGE II and SAGE III/ISS extinction spectra’, *Atmos. Meas. Tech.*,
883 17(7), pp. 2025–2054. Available at: <https://doi.org/10.5194/amt-17-2025-2024>.

884 Konopka, P. *et al.* (2022) ‘Stratospheric Moistening After 2000’, *Geophysical Research*
885 *Letters*, 49(8), p. e2021GL097609. Available at: <https://doi.org/10.1029/2021GL097609>.

886 Kovilakam, M., L. Thomason, and T. Knepp, 2023: SAGE III/ISS aerosol/cloud
887 categorization and its impact on GloSSAC, *Atmos. Meas. Tech.*, 16, 2709–2731.
888 <https://doi.org/10.5194/amt-16-2709-2023>.

889 Kramarova, N.A. *et al.* (2024) ‘2023 Antarctic Ozone Hole [in “State of the Climate in
890 2023”]’, *Bulletin of the American Meteorological Society*, 105(8), pp. S358–S361.
891 Available at: <https://doi.org/10.1175/BAMS-D-24-0099.1>.

892 Lawrence, Z.D. *et al.* (2020) ‘The Remarkably Strong Arctic Stratospheric Polar Vortex of
893 Winter 2020: Links to Record-Breaking Arctic Oscillation and Ozone Loss’, *Journal of*
894 *Geophysical Research: Atmospheres*, 125(22), p. e2020JD033271. Available at:
895 <https://doi.org/10.1029/2020JD033271>.

896 Leblanc, T. and McDermid, I.S. (2000) ‘Stratospheric ozone climatology from lidar
897 measurements at Table Mountain (34.4°N, 117.7°W) and Mauna Loa (19.5°N,
898 155.6°W)’, *Journal of Geophysical Research: Atmospheres*, 105(D11), pp. 14613–14623.
899 Available at: <https://doi.org/10.1029/2000JD900030>.

900 Lee, W.R. *et al.* (2021) ‘High-Latitude Stratospheric Aerosol Geoengineering Can Be More
901 Effective if Injection Is Limited to Spring’, *Geophysical Research Letters*, 48(9), p.
902 e2021GL092696. Available at: <https://doi.org/10.1029/2021GL092696>.

903 Legras, B. *et al.* (2022) ‘The evolution and dynamics of the Hunga Tonga–Hunga Ha’apai
904 sulfate aerosol plume in the stratosphere’, *Atmos. Chem. Phys.*, 22(22), pp. 14957–14970.
905 Available at: <https://doi.org/10.5194/acp-22-14957-2022>.

906 Li, B. *et al.* (2024) ‘CCl₄ emissions in eastern China during 2021–2022 and exploration of
907 potential new sources’, *Nature Communications*, 15(1), p. 1725. Available at:
908 <https://doi.org/10.1038/s41467-024-45981-x>.

909 Li, F., Austin, J. and Wilson, J. (2008) ‘The Strength of the Brewer–Dobson Circulation in a
910 Changing Climate: Coupled Chemistry–Climate Model Simulations’, *Journal of Climate*,

911 21(1), pp. 40–57. Available at: <https://doi.org/10.1175/2007JCLI1663.1>.

912 Li, Q. *et al.* (2005) ‘Convective outflow of South Asian pollution: A global CTM simulation
913 compared with EOS MLS observations’, *Geophysical Research Letters*, 32(14). Available
914 at: <https://doi.org/10.1029/2005GL022762>.

915 Lickley, M. *et al.* (2021) ‘Joint inference of CFC lifetimes and banks suggests previously
916 unidentified emissions’, *Nature Communications*, 12(1), p. 2920. Available at:
917 <https://doi.org/10.1038/s41467-021-23229-2>.

918 Lickley, M. *et al.* (2024) ‘The return to 1980 stratospheric halogen levels: A moving target in
919 ozone assessments from 2006 to 2022’, *EGUsphere*, 2024, pp. 1–30. Available at:
920 <https://doi.org/10.5194/egusphere-2024-1289>.

921 Lim, E.-P. *et al.* (2019) ‘Australian hot and dry extremes induced by weakenings of the
922 stratospheric polar vortex’, *Nature Geoscience*, 12(11), pp. 896–901. Available at:
923 <https://doi.org/10.1038/s41561-019-0456-x>.

924 Lim, E.-P. *et al.* (2021) ‘The 2019 Southern Hemisphere Stratospheric Polar Vortex
925 Weakening and Its Impacts’, *Bulletin of the American Meteorological Society*, 102(6), pp.
926 E1150–E1171. Available at: <https://doi.org/10.1175/BAMS-D-20-0112.1>.

927 Livesey, N.J., Santee, M.L. and Manney, G.L. (2015) ‘A Match-based approach to the
928 estimation of polar stratospheric ozone loss using Aura Microwave Limb Sounder
929 observations’, *Atmos. Chem. Phys.*, 15(17), pp. 9945–9963. Available at:
930 <https://doi.org/10.5194/acp-15-9945-2015>.

931 Loughman, R. *et al.* (2018) ‘The Ozone Mapping and Profiler Suite (OMPS) Limb Profiler
932 (LP) Version 1 aerosol extinction retrieval algorithm: theoretical basis’, *Atmos. Meas.
933 Tech.*, 11(5), pp. 2633–2651. Available at: <https://doi.org/10.1016/j.trac.2006.05.001>.

934 Madronich, S. *et al.* (1998) ‘Changes in biologically active ultraviolet radiation reaching the
935 Earth’s surface’, *Journal of Photochemistry and Photobiology B: Biology*, 46(1), pp. 5–
936 19. Available at: [https://doi.org/10.1016/S1011-1344\(98\)00182-1](https://doi.org/10.1016/S1011-1344(98)00182-1).

937 Mahieu, E. *et al.* (2014) ‘Recent Northern Hemisphere stratospheric HCl increase due to
938 atmospheric circulation changes’, *Nature*, 515(7525), pp. 104–107. Available at:
939 <https://doi.org/10.1038/nature13857>.

940 Maloney, C.M. *et al.* (2022) ‘The Climate and Ozone Impacts of Black Carbon Emissions
941 From Global Rocket Launches’, *Journal of Geophysical Research: Atmospheres*,
942 127(12), p. e2021JD036373. Available at: <https://doi.org/10.1029/2021JD036373>.

943 Manney, G.L. *et al.* (2011) ‘Unprecedented Arctic ozone loss in 2011’, *Nature*, 478(7370),
944 pp. 469–475. Available at: <https://doi.org/10.1038/nature10556>.

945 Manney, G.L. *et al.* (2020) ‘Record-low Arctic stratospheric ozone in 2020: MLS
946 observations of chemical processes and comparisons with previous extreme winters’,
947 *Geophysical Research Letters*, 47(16), p. e2020GL089063. Available at:
948 <https://doi.org/10.1029/2020GL089063>.

949 Manney, G.L. *et al.* (2022) ‘Signatures of Anomalous Transport in the 2019/2020 Arctic
950 Stratospheric Polar Vortex’, *Journal of Geophysical Research: Atmospheres*, 127(20), p.
951 e2022JD037407. Available at: <https://doi.org/10.1029/2022JD037407>.

952 Manney, G.L. *et al.* (2023) ‘Siege in the Southern Stratosphere: Hunga Tonga-Hunga Ha’apai
953 Water Vapor Excluded From the 2022 Antarctic Polar Vortex’, *Geophysical Research
954 Letters*, 50(14), p. e2023GL103855. Available at:
955 <https://doi.org/10.1029/2023GL103855>.

956 Marshall, L.R. *et al.* (2022) ‘Volcanic effects on climate: recent advances and future
957 avenues’, *Bulletin of Volcanology*, 84(5), p. 54. Available at:
958 <https://doi.org/10.1007/s00445-022-01559-3>.

959 Millán, L. *et al.* (2022) ‘The Hunga Tonga-Hunga Ha’apai Hydration of the Stratosphere’,

960 *Geophysical Research Letters*, 49(13), p. e2022GL099381. Available at:
961 <https://doi.org/10.1029/2022GL099381>.

962 Millán, L. *et al.* (2024) ‘The Evolution of the Hunga Hydration in a Moistening
963 Stratosphere’, *Geophysical Research Letters*, 51(19), p. e2024GL110841. Available at:
964 <https://doi.org/10.1029/2024GL110841>.

965 Minganti, D. *et al.* (2022) ‘Evaluation of the N₂O Rate of Change to Understand the
966 Stratospheric Brewer-Dobson Circulation in a Chemistry-Climate Model’, *Journal of*
967 *Geophysical Research: Atmospheres*, 127(22), p. e2021JD036390. Available at:
968 <https://doi.org/10.1029/2021JD036390>.

969 Mote, P.W. *et al.* (1996) ‘An atmospheric tape recorder: The imprint of tropical tropopause
970 temperatures on stratospheric water vapor’, *Journal of Geophysical Research:*
971 *Atmospheres*, 101(D2), pp. 3989–4006. Available at: <https://doi.org/10.1029/95JD03422>.

972 Müller, R. *et al.* (2005) ‘Impact of mixing and chemical change on ozone-tracer relations in
973 the polar vortex’, *Atmos. Chem. Phys.*, 5(11), pp. 3139–3151. Available at:
974 <https://doi.org/10.5194/acp-5-3139-2005>.

975 Murphy, D.M. *et al.* (2023) ‘Metals from spacecraft reentry in stratospheric aerosol
976 particles’, *Proceedings of the National Academy of Sciences*, 120(43), p. e2313374120.
977 Available at: <https://doi.org/10.1073/pnas.2313374120>.

978 Nassar, R. *et al.* (2006) ‘A global inventory of stratospheric chlorine in 2004’, *Journal of*
979 *Geophysical Research: Atmospheres*, 111(D22). Available at:
980 <https://doi.org/10.1029/2006JD007073>.

981 Nedoluha, G.E. *et al.* (2023) ‘Measurements of Stratospheric Water Vapor at Mauna Loa and
982 the Effect of the Hunga Tonga Eruption’, *Journal of Geophysical Research:*
983 *Atmospheres*, 128(8), p. e2022JD038100. Available at:
984 <https://doi.org/10.1029/2022JD038100>.

985 Oman, L.D. *et al.* (2010) ‘Multimodel assessment of the factors driving stratospheric ozone
986 evolution over the 21st century’, *Journal of Geophysical Research: Atmospheres*,
987 115(D24). Available at: <https://doi.org/10.1029/2010JD014362>.

988 Orbe, C. *et al.* (2020) ‘Mechanisms Linked to Recent Ozone Decreases in the Northern
989 Hemisphere Lower Stratosphere’, *Journal of Geophysical Research: Atmospheres*,
990 125(9), p. e2019JD031631. Available at: <https://doi.org/10.1029/2019JD031631>.

991 Ostler, A. *et al.* (2016) ‘Evaluation of column-averaged methane in models and TCCON with
992 a focus on the stratosphere’, *Atmos. Meas. Tech.*, 9(9), pp. 4843–4859. Available at:
993 <https://doi.org/10.5194/amt-9-4843-2016>.

994 Pan, L.L. *et al.* (2024) ‘East Asian summer monsoon delivers large abundances of very short-
995 lived organic chlorine substances to the lower stratosphere’, *Proceedings of the National*
996 *Academy of Sciences*, 121(12), p. e2318716121. Available at:
997 <https://doi.org/10.1073/pnas.2318716121>.

998 Park, M. *et al.* (2007) ‘Transport above the Asian summer monsoon anticyclone inferred
999 from Aura Microwave Limb Sounder tracers’, *Journal of Geophysical Research:*
1000 *Atmospheres*, 112(D16). Available at: <https://doi.org/10.1029/2006JD008294>.

1001 Park, M. *et al.* (2008) ‘Chemical isolation in the Asian monsoon anticyclone observed in
1002 Atmospheric Chemistry Experiment (ACE-FTS) data’, *Atmos. Chem. Phys.*, 8(3), pp.
1003 757–764. Available at: <https://doi.org/10.5194/acp-8-757-2008>.

1004 Pausas, J.G. and Keeley, J.E. (2021) ‘Wildfires and global change’, *Frontiers in Ecology and*
1005 *the Environment*, 19(7), pp. 387–395. Available at: <https://doi.org/10.1002/fee.2359>.

1006 Pitari, G. *et al.* (2014) ‘Stratospheric ozone response to sulfate geoengineering: Results from
1007 the Geoengineering Model Intercomparison Project (GeoMIP)’, *Journal of Geophysical*
1008 *Research: Atmospheres*, 119(5), pp. 2629–2653. Available at:

1009 <https://doi.org/10.1002/2013JD020566>.

1010 Prather, M.J., Froidevaux, L. and Livesey, N.J. (2023) ‘Observed changes in stratospheric
1011 circulation: decreasing lifetime of N₂O, 2005–2021’, *Atmos. Chem. Phys.*, 23(2), pp. 843–
1012 849. Available at: <https://doi.org/10.5194/acp-23-843-2023>.

1013 Prignon, M. *et al.* (2021) ‘Stratospheric fluorine as a tracer of circulation changes:
1014 comparison between infrared remote sensing observations and simulations with five
1015 modern reanalyses’, *Journal of Geophysical Research: Atmospheres*, 126(19), p.
1016 e2021JD034995. Available at: <https://doi.org/10.1029/2021JD034995>.

1017 Randel, W. and Park, M. (2019) ‘Diagnosing Observed Stratospheric Water Vapor
1018 Relationships to the Cold Point Tropical Tropopause’, *Journal of Geophysical Research:
1019 Atmospheres*, 124(13), pp. 7018–7033. Available at:
1020 <https://doi.org/10.1029/2019JD030648>.

1021 Randel, W.J. *et al.* (2010) ‘Asian Monsoon Transport of Pollution to the Stratosphere’,
1022 *Science*, 328(5978), pp. 611–613. Available at: <https://doi.org/10.1126/science.1182274>.

1023 Ravishankara, A.R., Daniel, J.S. and Portmann, R.W. (2009) ‘Nitrous oxide (N₂O): The
1024 dominant ozone-depleting substance emitted in the 21st century’, *Science*, 326(5949), pp.
1025 123–125. Available at: <https://doi.org/10.1126/science.1176985>.

1026 Revell, L.E. *et al.* (2012) ‘The sensitivity of stratospheric ozone changes through the 21st
1027 century to N₂O and CH₄’, *Atmos. Chem. Phys.*, 12(23), pp. 11309–11317. Available at:
1028 <https://doi.org/10.5194/acp-12-11309-2012>.

1029 Revell, L.E. *et al.* (2015) ‘The changing ozone depletion potential of N₂O in a future
1030 climate’, *Geophysical Research Letters*, 42(22), pp. 10047–10055. Available at:
1031 <https://doi.org/10.1002/2015GL065702>.

1032 Rex, M. *et al.* (2004) ‘Arctic ozone loss and climate change’, *Geophysical Research Letters*,
1033 31(4). Available at: <https://doi.org/10.1029/2003GL018844>.

1034 Rex, M. *et al.* (2006) ‘Arctic winter 2005: Implications for stratospheric ozone loss and
1035 climate change’, *Geophysical Research Letters*, 33(23). Available at:
1036 <https://doi.org/10.1029/2006GL026731>.

1037 Rieger, L.A. *et al.* (2021) ‘Stratospheric temperature and ozone anomalies associated with the
1038 2020 Australian New Year fires’, *Geophysical Research Letters*, 48(24), p.
1039 e2021GL095898. Available at: <https://doi.org/10.1029/2021GL095898>.

1040 Robrecht, S. *et al.* (2021) ‘Potential of future stratospheric ozone loss in the midlatitudes
1041 under global warming and sulfate geoengineering’, *Atmos. Chem. Phys.*, 21(4), pp. 2427–
1042 2455. Available at: <https://doi.org/10.5194/acp-21-2427-2021>.

1043 Ross, M., Mills, M. and Toohey, D. (2010) ‘Potential climate impact of black carbon emitted
1044 by rockets’, *Geophysical Research Letters*, 37(24). Available at:
1045 <https://doi.org/10.1029/2010GL044548>.

1046 Safieddine, S. *et al.* (2020) ‘Antarctic Ozone Enhancement During the 2019 Sudden
1047 Stratospheric Warming Event’, *Geophysical Research Letters*, 47(14), p.
1048 e2020GL087810. Available at: <https://doi.org/10.1029/2020GL087810>.

1049 Salawitch, R.J. *et al.* (2002) ‘Chemical loss of ozone during the Arctic winter of 1999/2000:
1050 An analysis based on balloon-borne observations’, *Journal of Geophysical Research:
1051 Atmospheres*, 107(D20), p. SOL 11-1-SOL 11-20. Available at:
1052 <https://doi.org/10.1029/2001JD000620>.

1053 Salawitch, R.J. and McBride, L.A. (2022) ‘Australian wildfires depleted the ozone layer’,
1054 *Science*, 378(6622), pp. 829–830. Available at: <https://doi.org/10.1126/science.add2056>.

1055 Santee, M.L. *et al.* (2017) ‘A comprehensive overview of the climatological composition of
1056 the Asian summer monsoon anticyclone based on 10 years of Aura Microwave Limb
1057 Sounder measurements’, *Journal of Geophysical Research: Atmospheres*, 122(10), pp.

1058 5491–5514. Available at: <https://doi.org/10.1002/2016JD026408>.

1059 Santee, M.L. *et al.* (2022) ‘Prolonged and pervasive perturbations in the composition of the
 1060 Southern Hemisphere midlatitude lower stratosphere from the Australian New Year’s
 1061 fires’, *Geophysical Research Letters*, 49(4), p. e2021GL096270. Available at:
 1062 <https://doi.org/10.1029/2021GL096270>.

1063 Santee, M.L. *et al.* (2023) ‘Strong Evidence of Heterogeneous Processing on Stratospheric
 1064 Sulfate Aerosol in the Extrapolar Southern Hemisphere Following the 2022 Hunga
 1065 Tonga-Hunga Ha’apai Eruption’, *Journal of Geophysical Research: Atmospheres*,
 1066 128(16), p. e2023JD039169. Available at: <https://doi.org/10.1029/2023JD039169>.

1067 Santee, M.L. *et al.* (2024) ‘The Influence of Stratospheric Hydration From the Hunga
 1068 Eruption on Chemical Processing in the 2023 Antarctic Vortex’, *Journal of Geophysical
 1069 Research: Atmospheres*, 129(16), p. e2023JD040687. Available at:
 1070 <https://doi.org/10.1029/2023JD040687>.

1071 Santer, B.D. *et al.* (2001) ‘Accounting for the effects of volcanoes and ENSO in comparisons
 1072 of modeled and observed temperature trends’, *Journal of Geophysical Research:
 1073 Atmospheres*, 106(D22), pp. 28033–28059. Available at:
 1074 <https://doi.org/10.1029/2000JD000189>.

1075 Schoeberl, M.R. *et al.* (2022) ‘Analysis and Impact of the Hunga Tonga-Hunga Ha’apai
 1076 Stratospheric Water Vapor Plume’, *Geophysical Research Letters*, 49(20), p.
 1077 e2022GL100248. Available at: <https://doi.org/10.1029/2022GL100248>.

1078 Schoeberl, M.R. *et al.* (2023) ‘The Estimated Climate Impact of the Hunga Tonga-Hunga
 1079 Ha’apai Eruption Plume’, *Geophysical Research Letters*, 50(18), p. e2023GL104634.
 1080 Available at: <https://doi.org/10.1029/2023GL104634>.

1081 Schwartz, M.J. *et al.* (2020) ‘Australian New Year’s PyroCb impact on stratospheric
 1082 composition’, *Geophysical Research Letters*, 47(24), p. e2020GL090831. Available at:
 1083 <https://doi.org/10.1029/2020GL090831>.

1084 Sciences, N.A. of (2015) *Climate Intervention: Reflecting Sunlight to Cool Earth*.
 1085 Washington, DC: The National Academies Press. Available at:
 1086 <https://doi.org/10.17226/18988>.

1087 Sciences, N.A. of (2021) *Reflecting Sunlight: Recommendations for Solar Geoengineering
 1088 Research and Research Governance*. Washington, DC: The National Academies Press.
 1089 Available at: <https://doi.org/10.17226/25762>.

1090 Sellitto, P. *et al.* (2022) ‘The unexpected radiative impact of the Hunga Tonga eruption of
 1091 15th January 2022’, *Communications Earth & Environment*, 3(1), p. 288. Available at:
 1092 <https://doi.org/10.1038/s43247-022-00618-z>.

1093 Smalley, K.M. *et al.* (2017) ‘Contribution of different processes to changes in tropical lower-
 1094 stratospheric water vapor in chemistry–climate models’, *Atmos. Chem. Phys.*, 17(13), pp.
 1095 8031–8044. Available at: <https://doi.org/10.5194/acp-17-8031-2017>.

1096 Smoydzin, L. and Hoor, P. (2022) ‘Contribution of Asian emissions to upper tropospheric
 1097 CO over the remote Pacific’, *Atmos. Chem. Phys.*, 22(11), pp. 7193–7206. Available at:
 1098 <https://doi.org/10.5194/acp-22-7193-2022>.

1099 Solomon, S. *et al.* (2010) ‘Contributions of Stratospheric Water Vapor to Decadal Changes in
 1100 the Rate of Global Warming’, *Science*, 327(5970), pp. 1219–1223. Available at:
 1101 <https://doi.org/10.1126/science.1182488>.

1102 Solomon, S. *et al.* (2011) ‘The Persistently Variable “Background” Stratospheric Aerosol
 1103 Layer and Global Climate Change’, *Science*, 333(6044), pp. 866–870. Available at:
 1104 <https://doi.org/10.1126/science.1206027>.

1105 Solomon, S. *et al.* (2016) ‘Emergence of healing in the Antarctic ozone layer’, *Science*,
 1106 353(6296), pp. 269–274. Available at: <https://doi.org/10.1126/science.aae0061>.

- 1107 Solomon, S. *et al.* (2023) ‘Chlorine activation and enhanced ozone depletion induced by
1108 wildfire aerosol’, *Nature*, 615(7951), pp. 259–264. Available at:
1109 <https://doi.org/10.1038/s41586-022-05683-0>.
- 1110 Stauffer, R.M. *et al.* (2022) ‘An Examination of the Recent Stability of Ozone Global
1111 Network Data’, *Earth and Space Science*, 9(10), p. e2022EA002459. Available at:
1112 <https://doi.org/10.1029/2022EA002459>.
- 1113 Steinbrecht, W. *et al.* (2023) ‘Long-Term Monitoring of the Stratosphere by Lidars in the
1114 Network for the Detection of Atmospheric Composition Change BT - Proceedings of the
1115 30th International Laser Radar Conference’, in J.T. Sullivan *et al.* (eds). Cham: Springer
1116 International Publishing, pp. 877–883.
- 1117 Stone, K.A. *et al.* (2017) ‘Observing the Impact of Calbuco Volcanic Aerosols on South
1118 Polar Ozone Depletion in 2015’, *Journal of Geophysical Research: Atmospheres*,
1119 122(21), pp. 11862–11879. Available at: <https://doi.org/10.1002/2017JD026987>.
- 1120 Strahan, S.E. *et al.* (2020) ‘Observed Hemispheric Asymmetry in Stratospheric Transport
1121 Trends From 1994 to 2018’, *Geophysical Research Letters*, 47(17), p. e2020GL088567.
1122 Available at: <https://doi.org/10.1029/2020GL088567>.
- 1123 Strahan, S.E. *et al.* (2022) ‘Unexpected repartitioning of stratospheric inorganic chlorine after
1124 the 2020 Australian wildfires’, *Geophysical Research Letters*, 49(14), p.
1125 e2022GL098290. Available at: <https://doi.org/10.1029/2022GL098290>.
- 1126 Taha, G. *et al.* (2022) ‘Tracking the 2022 Hunga Tonga-Hunga Ha’apai Aerosol Cloud in the
1127 Upper and Middle Stratosphere Using Space-Based Observations’, *Geophysical Research
1128 Letters*, 49(19), p. e2022GL100091. Available at:
1129 <https://doi.org/10.1029/2022GL100091>.
- 1130 Tao, M. *et al.* (2023) ‘Multi-decadal variability controls short-term stratospheric water vapor
1131 trends’, *Communications Earth & Environment*, 4(1), p. 441. Available at:
1132 <https://doi.org/10.1038/s43247-023-01094-9>.
- 1133 Tegtmeier, S. *et al.* (2008) ‘Relative importance of dynamical and chemical contributions to
1134 Arctic wintertime ozone’, *Geophysical Research Letters*, 35(17). Available at:
1135 <https://doi.org/10.1029/2008GL034250>.
- 1136 Thomason, L. W. and Coauthors, 2018: A global space-based stratospheric aerosol
1137 climatology: 1979–2016, *Earth Syst. Sci. Data*, 10, 469–492,
1138 <https://doi.org/10.5194/essd-10-469-2018>.
- 1139 Thompson, A.M. *et al.* (2004) ‘SHADOZ—A Tropical Ozone Global Network
1140 for the Atmospheric Community’, *Bulletin of the American Meteorological Society*,
1141 85(10), pp. 1549–1564. Available at: <https://doi.org/10.1175/BAMS-85-10-1549>.
- 1142 Thompson, D.W.J. *et al.* (2009) ‘Identifying Signatures of Natural Climate Variability in
1143 Time Series of Global-Mean Surface Temperature: Methodology and Insights’, *Journal
1144 of Climate*, 22(22), pp. 6120–6141. Available at:
1145 <https://doi.org/10.1175/2009JCLI3089.1>.
- 1146 Tilmes, S. *et al.* (2004) ‘Ozone loss and chlorine activation in the Arctic winters 1991–2003
1147 derived with the tracer-tracer correlations’, *Atmospheric Chemistry and Physics*, 4(8), pp.
1148 2181–2213. Available at: <https://doi.org/10.5194/acp-4-2181-2004>.
- 1149 Tilmes, S. *et al.* (2006) ‘Chemical ozone loss in the Arctic and Antarctic stratosphere
1150 between 1992 and 2005’, *Geophysical Research Letters*, 33(20). Available at:
1151 <https://doi.org/10.1029/2006GL026925>.
- 1152 Tilmes, S. *et al.* (2012) ‘Impact of very short-lived halogens on stratospheric ozone
1153 abundance and UV radiation in a geo-engineered atmosphere’, *Atmos. Chem. Phys.*,
1154 12(22), pp. 10945–10955. Available at: <https://doi.org/10.5194/acp-12-10945-2012>.
- 1155 Tilmes, S. *et al.* (2024) ‘Research criteria towards an interdisciplinary Stratospheric Aerosol

- 1156 Intervention assessment’, *Oxford Open Climate Change*, 4(1), p. kgae010. Available at:
1157 <https://doi.org/10.1093/oxfclm/kgae010>.
- 1158 Tilmes, S., Müller, R. and Salawitch, R. (2008) ‘The Sensitivity of Polar Ozone Depletion to
1159 Proposed Geoengineering Schemes’, *Science*, 320(5880), pp. 1201–1204. Available at:
1160 <https://doi.org/10.1126/science.1153966>.
- 1161 Villamayor, J. *et al.* (2023) ‘Very short-lived halogens amplify ozone depletion trends in the
1162 tropical lower stratosphere’, *Nature Climate Change*, 13(6), pp. 554–560. Available at:
1163 <https://doi.org/10.1038/s41558-023-01671-y>.
- 1164 Vömel, H., Evan, S. and Tully, M. (2022) ‘Water vapor injection into the stratosphere by
1165 Hunga Tonga-Hunga Ha’apai’, *Science*, 377(6613), pp. 1444–1447. Available at:
1166 <https://doi.org/10.1126/science.abq2299>.
- 1167 von der Gathen, P. *et al.* (2021) ‘Climate change favours large seasonal loss of Arctic ozone’,
1168 *Nature Communications*, 12(1). Available at: [https://doi.org/10.1038/s41467-021-24089-](https://doi.org/10.1038/s41467-021-24089-6)
1169 6.
- 1170 Wang, H.J.R. *et al.* (2020) ‘Validation of SAGE III/ISS Solar Occultation Ozone Products
1171 With Correlative Satellite and Ground-Based Measurements’, *Journal of Geophysical*
1172 *Research: Atmospheres*, 125(11), p. e2020JD032430. Available at:
1173 <https://doi.org/10.1029/2020JD032430>.
- 1174 Wang, X. *et al.* (2023) ‘Stratospheric Climate Anomalies and Ozone Loss Caused by the
1175 Hunga Tonga-Hunga Ha’apai Volcanic Eruption’, *Journal of Geophysical Research:*
1176 *Atmospheres*, 128(22), p. e2023JD039480. Available at:
1177 <https://doi.org/10.1029/2023JD039480>.
- 1178 Wargan, K. *et al.* (2018) ‘Recent Decline in Extratropical Lower Stratospheric Ozone
1179 Attributed to Circulation Changes’, *Geophysical Research Letters*, 45(10), pp. 5166–
1180 5176. Available at: <https://doi.org/10.1029/2018GL077406>.
- 1181 Wargan, K. *et al.* (2020) ‘The anomalous 2019 Antarctic ozone hole in the GEOS constituent
1182 data assimilation system with MLS observations’, *Journal of Geophysical Research:*
1183 *Atmospheres*, 125(18), p. e2020JD033335. Available at:
1184 <https://doi.org/10.1029/2020JD033335>.
- 1185 Wargan, K. *et al.* (2023) ‘M2-SCREAM: A Stratospheric Composition Reanalysis of Aura
1186 MLS Data With MERRA-2 Transport’, *Earth and Space Science*, 10(2), p.
1187 e2022EA002632. Available at: <https://doi.org/10.1029/2022EA002632>.
- 1188 Waters, J.W. *et al.* (2006) ‘The Earth observing system microwave limb sounder (EOS MLS)
1189 on the aura Satellite’, *IEEE Transactions on Geoscience and Remote Sensing*, 44(5), pp.
1190 1075–1092. Available at: <https://doi.org/10.1109/TGRS.2006.873771>.
- 1191 Weber, M. *et al.* (2011) ‘The Brewer-Dobson circulation and total ozone from seasonal to
1192 decadal time scales’, *Atmospheric Chemistry and Physics*, 11(21), pp. 11221–11235.
1193 Available at: <https://doi.org/10.5194/acp-11-11221-2011>.
- 1194 Weber, M. *et al.* (2022) ‘Global total ozone recovery trends attributed to ozone-depleting
1195 substance (ODS) changes derived from five merged ozone datasets’, *Atmos. Chem. Phys.*,
1196 22(10), pp. 6843–6859. Available at: <https://doi.org/10.5194/acp-22-6843-2022>.
- 1197 Western, L.M. *et al.* (2023) ‘Global increase of ozone-depleting chlorofluorocarbons from
1198 2010 to 2020’, *Nature Geoscience*, 16(4), pp. 309–313. Available at:
1199 <https://doi.org/10.1038/s41561-023-01147-w>.
- 1200 Wilmouth, D.M. *et al.* (2023) ‘Impact of the Hunga Tonga volcanic eruption on stratospheric
1201 composition’, *Proceedings of the National Academy of Sciences*, 120(46), p.
1202 e2301994120. Available at: <https://doi.org/10.1073/pnas.2301994120>.
- 1203 Witze, A. (2022) ‘Why the Tongan volcanic eruption was so shocking’, *Nature*, pp. 376–378.
1204 Available at: <https://doi.org/10.1038/d41586-022-00394-y>.

- 1205 WMO (2022) *World Meteorological Organization (WMO). Executive Summary. Scientific*
1206 *Assessment of Ozone Depletion: 2022, GAW Report No. 578*. Geneva, Switzerland.
- 1207 Wohltmann, I. *et al.* (2020) ‘Near-Complete Local Reduction of Arctic Stratospheric Ozone
1208 by Severe Chemical Loss in Spring 2020’, *Geophysical Research Letters*, 47(20), p.
1209 e2020GL089547. Available at: <https://doi.org/10.1029/2020GL089547>.
- 1210 Wohltmann, I. *et al.* (2024) ‘The Chemical Effect of Increased Water Vapor From the Hunga
1211 Tonga-Hunga Ha’apai Eruption on the Antarctic Ozone Hole’, *Geophysical Research*
1212 *Letters*, 51(4), p. e2023GL106980. Available at: <https://doi.org/10.1029/2023GL106980>.
- 1213 Xu, J. *et al.* (2022) ‘Large amounts of water vapor were injected into the stratosphere by the
1214 Hunga Tonga–Hunga Ha’apai volcano eruption’, *Atmosphere*. Available at:
1215 <https://doi.org/10.3390/atmos13060912>.
- 1216 Yook, S., Thompson, D.W.J. and Solomon, S. (2022) ‘Climate Impacts and Potential Drivers
1217 of the Unprecedented Antarctic Ozone Holes of 2020 and 2021’, *Geophysical Research*
1218 *Letters*, 49(10), p. e2022GL098064. Available at:
1219 <https://doi.org/10.1029/2022GL098064>.
- 1220 Zhang, J. *et al.* (2023) ‘Potential Impacts on Ozone and Climate From a Proposed Fleet of
1221 Supersonic Aircraft’, *Earth’s Future*, 11(4), p. e2022EF003409. Available at:
1222 <https://doi.org/10.1029/2022EF003409>.
- 1223 Zhang, J. *et al.* (2024) ‘Stratospheric Chlorine Processing After the Unprecedented Hunga
1224 Tonga Eruption’, *Geophysical Research Letters*, 51(17), p. e2024GL108649. Available
1225 at: <https://doi.org/10.1029/2024GL108649>.
- 1226 Zhou, X. *et al.* (2024) ‘Antarctic Vortex Dehydration in 2023 as a Substantial Removal
1227 Pathway for Hunga Tonga-Hunga Ha’apai Water Vapor’, *Geophysical Research Letters*,
1228 51(8), p. e2023GL107630. Available at: <https://doi.org/10.1029/2023GL107630>.
- 1229 Zhu, Y. *et al.* (2018) ‘Stratospheric aerosols, polar stratospheric clouds, and polar ozone
1230 depletion after the Mount Calbuco Eruption in 2015’, *Journal of Geophysical Research:*
1231 *Atmospheres*, 123(21), pp. 12,308–312,331. Available at:
1232 <https://doi.org/10.1029/2018JD028974>.
- 1233 Zhu, Y. *et al.* (2022) ‘Perturbations in stratospheric aerosol evolution due to the water-rich
1234 plume of the 2022 Hunga-Tonga eruption’, *Communications Earth & Environment*, 3(1),
1235 p. 248. Available at: <https://doi.org/10.1038/s43247-022-00580-w>.
- 1236 Zhu, Y. *et al.* (2023) ‘Stratospheric ozone depletion inside the volcanic plume shortly after
1237 the 2022 Hunga Tonga eruption’, *Atmos. Chem. Phys.*, 23(20), pp. 13355–13367.
1238 Available at: <https://doi.org/10.5194/acp-23-13355-2023>.